Excem Research Papers in Electronics and Electromagnetics

Number 3 April 2021 ISBN 978-2-909056-23-4

Some Results on Power in Passive Linear Time-Invariant Multiports, Part 2

FRÉDÉRIC BROYDÉ[1], and
EVELYNE CLAVELIER[2]

[1]Excem, 12 chemin des Hauts de Clairefontaine, 78580 Maule, France
[2]Eurexcem, 12 chemin des Hauts de Clairefontaine, 78580 Maule, France

Corresponding author: Frédéric Broydé (e-mail: fredbroyde@eurexcem.com).

ABSTRACT We investigate the transfer of power between two passive linear time-invariant multiports having the same number of ports, in the harmonic steady state. One of the multiports is a generator in a configuration A, or a load in a configuration B. The other multiport is a load in configuration A, or a generator in configuration B. We define the power transfer ratios in these configurations. A new reciprocal theorem on the power transfer ratios relates the extrema of the power transfer ratios obtained for all nonzero excitations, in the two configurations. We define a power match figure, which is a new metric of the power transfer ratios. It is equal to the return figure under appropriate assumptions. We also study some upper bounds on the return figure, and show that, for arbitrary excitations, the absolute values of the entries of the scattering matrix do not sufficiently characterize the power transfer ratios. We apply this theory to a multiport antenna array and to a passive MIMO device.

INDEX TERMS Power transfer, power transfer ratio, return figure, scattering parameters.

I. INTRODUCTION

This article is a sequel of [1], which was a revised and expanded version of the material presented in [2]–[3]. In what follows, [1] is referred to as "Part 1", and the numbering of lemmas, theorems, etc, is a continuation of the numbering used in Part 1. However, no prior knowledge of Part 1 is necessary to read what follows.

Let us consider two linear time-invariant (LTI) circuits, referred to as "configurations", operating in the harmonic steady state, at a given frequency. The two configurations are shown in Fig. 1. In configuration A (CA), an LTI single-port generator of internal impedance Z_{GA} is connected to an LTI single-port load of impedance Z_{GB}. In configuration B (CB), an LTI single-port generator of internal impedance Z_{GB} is connected to an LTI single-port load of impedance Z_{GA}. Let us use:

- P_{AAVG} to denote the average power available from the generator, in CA;
- P_{ADG} to denote the average power delivered by the generator, in CA;
- P_{BAVG} to denote the average power available from the generator, in CB; and
- P_{BDG} to denote the average power delivered by the generator, in CB.

To ensure that P_{AAVG} and P_{BAVG} are defined, we assume that the real parts of Z_{GA} and Z_{GB} are both positive. Assuming nonzero P_{AAVG} and P_{BAVG}, we can define the power transfer ratio in CA, given by $t_A = P_{ADG}/P_{AAVG}$, and the power transfer ratio in CB, given by $t_B = P_{BDG}/P_{BAVG}$. Power conservation entails $0 \leqslant t_A \leqslant 1$ and $0 \leqslant t_B \leqslant 1$. Ignoring noise power contributions, we find

$$t_A = \frac{4\mathrm{Re}(Z_{GA})\mathrm{Re}(Z_{GB})}{|Z_{GA}+Z_{GB}|^2} = t_B\,, \tag{1}$$

where $\mathrm{Re}(z)$ denotes the real part of a complex number z. Let $\bar{z}$ denote the complex conjugate of a complex number z. It follows from (1) that $t_A = t_B = 1$ if and only if $Z_{GB} = \overline{Z_{GA}}$, in line with the maximum power transfer theorem [4, Sec. 7.4]–[5, Sec. 11.1]. It is shown in Appendix A that t_A and t_B are the "power transmission coefficients" defined in [6, Sec. III], in connection with the use of power waves to prove $t_A = t_B$.

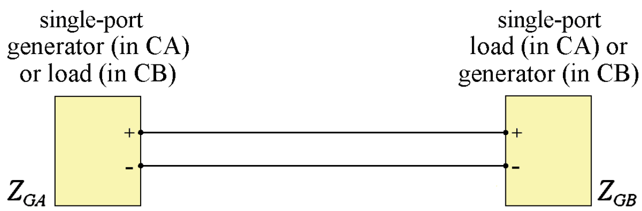

FIGURE 1. The two configurations, CA and CB, considered in the introduction.

This article is about the power transfer ratios relevant to passive LTI multiports. Section II provides elementary definitions and properties of the power transfer ratios t_A and t_B applicable to a multiport generator and a multiport load. Here, t_A and t_B are functions of the applicable excitations, and they need not be equal. In Section III, a new theoretical development allows us to extend (1) to multiports, in the form of a reciprocal theorem on the power transfer ratios. This development is discussed in Section IV. To obtain a suitable metric of the power transfer ratios when the excitations are not known, we use the new reciprocal theorem to define the power match figure, in Section V. We show that, under suitable assumptions, the power match figure is equal to the return figure introduced and used in [7]–[11].

In Section VI, we show that the absolute values of the entries of the scattering matrix do not determine the return figure, and that it is nevertheless possible to compute three upper bounds on the return figure, these upper bounds being solely derived from the absolute values of the entries of the scattering matrix.

Our results are applied to a multiport antenna array (MAA) in Section VII. In this case, in contrast to the absolute values of the entries of the scattering matrix, the return figure characterizes the lowest possible power transfer ratios during MIMO radio transmission. Other parameters that have been introduced to characterize matching to a MAA [12]-[17] are discussed in Section VII. Our results are also applied to a passive multiple-input-port and multiple-output-port (MIMO) device, in Section VIII and Section IX.

II. THE POWER TRANSFER RATIOS

Let N be a positive integer. In what follows, when we say that a first N-port device is connected to a second N-port device, it is assumed that: the ports of the first N-port device are numbered from 1 to N; the ports of the second N-port device are numbered from 1 to N; and, for any integer $p \in \{1, \dots, N\}$, port p of the first N-port device is connected to port p of the second N-port device (positive terminal to positive terminal and negative terminal to negative terminal).

We consider two LTI circuits, referred to as "configurations", operating in the harmonic steady state, at a given frequency f_G. The two configurations are shown in Fig. 2. In configuration A (CA), an LTI N-port generator, of internal impedance matrix $\mathbf{Z}_{GA}$ at f_G, is connected to an LTI N-port load of impedance matrix $\mathbf{Z}_{GB}$ at f_G. In configuration B (CB), an LTI N-port generator, of internal impedance matrix $\mathbf{Z}_{GB}$ at f_G, is connected to an LTI N-port load of impedance matrix $\mathbf{Z}_{GA}$ at f_G. The matrices $\mathbf{Z}_{GB}$ and $\mathbf{Z}_{GA}$ are of size N by N. Let us use:

- P_{AAVG} to denote the average power available from the N-port generator, in CA;
- P_{ADG} to denote the average power delivered by the N-port generator, in CA;
- P_{BAVG} to denote the average power available from the N-port generator, in CB; and
- P_{BDG} to denote the average power delivered by the N-port generator, in CB.

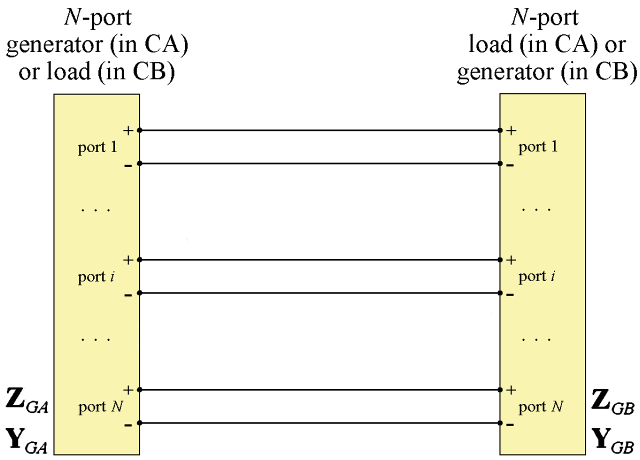

FIGURE 2. The two configurations, CA and CB, considered in Section II.

We use $\mathbf{M}^*$ to denote the hermitian adjoint of an arbitrary complex matrix $\mathbf{M}$. Recall that, if $\mathbf{M}$ is square, the hermitian part of $\mathbf{M}$, denoted by $H(\mathbf{M})$, is the matrix given by

$$H(\mathbf{M}) = \frac{\mathbf{M} + \mathbf{M}^*}{2} \, . \tag{2}$$

We assume that $H(\mathbf{Z}_{GA})$ and $H(\mathbf{Z}_{GB})$ are positive definite, so that they are invertible by [18, Sec. 7.1.7]. This ensures that P_{AAVG} and P_{BAVG} are defined and given by [19]:

$$P_{AAVG} = \frac{1}{2} \mathbf{V}_{OGA}^* \left(\mathbf{Z}_{GA} + \mathbf{Z}_{GA}^* \right)^{-1} \mathbf{V}_{OGA} \tag{3}$$

and

$$P_{BAVG} = \frac{1}{2} \mathbf{V}_{OGB}^* \left(\mathbf{Z}_{GB} + \mathbf{Z}_{GB}^* \right)^{-1} \mathbf{V}_{OGB} \, , \tag{4}$$

where $\mathbf{V}_{OGA}$ is the column vector of the rms open-circuit voltages of the N-port generator in CA, $\mathbf{V}_{OGB}$ is the column vector of the rms open-circuit voltages of the N-port generator in CB, and where we have ignored noise power contributions.

We are going to use several times Lemma 1, which was stated and proven in Part 1, section II. It tells us that, if $\mathbf{M}$ is a square complex matrix such that $H(\mathbf{M})$ is positive definite, then $\mathbf{M}$ is invertible and $H(\mathbf{M}^{-1})$ is positive definite. By Lemma 1, we can define $\mathbf{Y}_{GA} = \mathbf{Z}_{GA}^{-1}$ and $\mathbf{Y}_{GB} = \mathbf{Z}_{GB}^{-1}$, the hermitian parts of $\mathbf{Y}_{GA}$ and $\mathbf{Y}_{GB}$ being both positive definite. It also follows from Lemma 1 that, instead of assuming that $\mathbf{Z}_{GA}$ and $\mathbf{Z}_{GB}$ exist and that $H(\mathbf{Z}_{GA})$ and $H(\mathbf{Z}_{GB})$ are positive definite, we could equivalently have assumed that $\mathbf{Y}_{GA}$ and $\mathbf{Y}_{GB}$ exist and that $H(\mathbf{Y}_{GA})$ and $H(\mathbf{Y}_{GB})$ are positive definite. We have

$$P_{AAVG} = \frac{1}{2} \mathbf{I}_{SGA}^* \left(\mathbf{Y}_{GA} + \mathbf{Y}_{GA}^* \right)^{-1} \mathbf{I}_{SGA} \tag{5}$$

and

$$P_{BAVG} = \frac{1}{2} \mathbf{I}_{SGB}^* \left(\mathbf{Y}_{GB} + \mathbf{Y}_{GB}^* \right)^{-1} \mathbf{I}_{SGB} \, , \tag{6}$$

where $\mathbf{I}_{SGA}$ is the column vector of the rms short-circuit currents of the N-port generator in CA, $\mathbf{I}_{SGB}$ is the column vector of the rms short-circuit currents of the N-port generator in CB, and where we have ignored noise power contributions.

$H(\mathbf{Z}_{GA})$ and $H(\mathbf{Y}_{GA})$ being positive definite, it follows from (3) and (5) that P_{AAVG} is nonzero if and only if $\mathbf{I}_{SGA}$ is nonzero, or, equivalently, if and only if $\mathbf{V}_{OGA}$ is nonzero. In this case, we can define the power transfer ratio in CA, given by

$$t_A = \frac{P_{ADG}}{P_{AAVG}} \,. \tag{7}$$

$H(\mathbf{Z}_{GB})$ and $H(\mathbf{Y}_{GB})$ being positive definite, if follows from (4) and (6) that P_{BAVG} is nonzero if and only if $\mathbf{I}_{SGB}$ is nonzero, or, equivalently, if and only if $\mathbf{V}_{OGB}$ is nonzero. In this case, we can define the power transfer ratio in CB, given by

$$t_B = \frac{P_{BDG}}{P_{BAVG}} \,. \tag{8}$$

The definition of the available power entails $P_{ADG} \leqslant P_{AAVG}$ and $P_{BDG} \leqslant P_{BAVG}$, so that

$$0 \leqslant t_A \leqslant 1 \tag{9}$$

and

$$0 \leqslant t_B \leqslant 1 \,. \tag{10}$$

Ignoring noise power contributions, we find by inspection that

$$P_{ADG} = \mathbf{I}_{SGA}^* \mathbf{Z}_{PAB}^* \frac{\mathbf{Y}_{GB} + \mathbf{Y}_{GB}^*}{2} \mathbf{Z}_{PAB} \mathbf{I}_{SGA} \tag{11}$$

and

$$P_{BDG} = \mathbf{I}_{SGB}^* \mathbf{Z}_{PAB}^* \frac{\mathbf{Y}_{GA} + \mathbf{Y}_{GA}^*}{2} \mathbf{Z}_{PAB} \mathbf{I}_{SGB} \,, \tag{12}$$

where

$$\mathbf{Z}_{PAB} = (\mathbf{Y}_{GA} + \mathbf{Y}_{GB})^{-1} \tag{13}$$

is defined because $H(\mathbf{Y}_{GA} + \mathbf{Y}_{GB}) = H(\mathbf{Y}_{GA}) + H(\mathbf{Y}_{GB})$ is positive definite by [18, Sec. 7.1.3], so that we can use Lemma 1 again. Thus, the power transfer ratios in CA and CB are given by

$$t_A = \frac{\mathbf{I}_{SGA}^* \mathbf{Z}_{PAB}^* (\mathbf{Y}_{GB} + \mathbf{Y}_{GB}^*) \mathbf{Z}_{PAB} \mathbf{I}_{SGA}}{\mathbf{I}_{SGA}^* (\mathbf{Y}_{GA} + \mathbf{Y}_{GA}^*)^{-1} \mathbf{I}_{SGA}} \tag{14}$$

and

$$t_B = \frac{\mathbf{I}_{SGB}^* \mathbf{Z}_{PAB}^* (\mathbf{Y}_{GA} + \mathbf{Y}_{GA}^*) \mathbf{Z}_{PAB} \mathbf{I}_{SGB}}{\mathbf{I}_{SGB}^* (\mathbf{Y}_{GB} + \mathbf{Y}_{GB}^*)^{-1} \mathbf{I}_{SGB}} \,. \tag{15}$$

Since (14) and (15) depend on $\mathbf{I}_{SGA}$ and $\mathbf{I}_{SGB}$, respectively, we have found that t_A and t_B are functions of the applicable excitations, so that, if $N \geqslant 2$, they need not be equal. Thus, (1) cannot apply to $N \geqslant 2$. Consequently, some work is needed to generalize (1) to any positive N.

Let $||\mathbf{x}||_2 = \sqrt{\mathbf{x}^* \mathbf{x}}$ be the euclidian vector norm of an arbitrary complex column vector $\mathbf{x}$. We use $\mathbb{S}_N$ to denote the hypersphere of the unit vectors of $\mathbb{C}^N$. For a fixed $\mathbf{I}_{SGA}/||\mathbf{I}_{SGA}||_2$, (14) shows that t_A does not depend on $||\mathbf{I}_{SGA}||_2$. Thus, the set of the possible values of t_A is determined by $\mathbf{Y}_{GA}$, $\mathbf{Y}_{GB}$ and the set of the possible values of $\mathbf{I}_{SGA}/||\mathbf{I}_{SGA}||_2$ for $\mathbf{I}_{SGA} \neq \mathbf{0}$, which is a subset of $\mathbb{S}_N$. If we have no better information on the set of the possible values of $\mathbf{I}_{SGA}/||\mathbf{I}_{SGA}||_2$, we may have to assume that $\mathbf{I}_{SGA}/||\mathbf{I}_{SGA}||_2$ may lie anywhere in $\mathbb{S}_N$.

Likewise, for a fixed $\mathbf{I}_{SGB}/||\mathbf{I}_{SGB}||_2$, (15) shows that t_B does not depend on $||\mathbf{I}_{SGB}||_2$. Thus, the set of the possible values of t_B is determined by $\mathbf{Y}_{GA}$, $\mathbf{Y}_{GB}$ and the set of the possible values of $\mathbf{I}_{SGB}/||\mathbf{I}_{SGB}||_2$ for $\mathbf{I}_{SGB} \neq \mathbf{0}$, which is a subset of $\mathbb{S}_N$. If we have no better information on the set of the possible values of $\mathbf{I}_{SGB}/||\mathbf{I}_{SGB}||_2$, we may have to assume that $\mathbf{I}_{SGB}/||\mathbf{I}_{SGB}||_2$ may lie anywhere in $\mathbb{S}_N$.

III. THEOREMS ON THE POWER TRANSFER RATIOS

To prove the next theorem, we are going to need the following result:

Lemma 3. Let $\mathbf{A}$ and $\mathbf{B}$ be two square complex matrices of the same size, such that $\mathbf{A} + \mathbf{B}$ is invertible. Let

$$\mathbf{K} = (\mathbf{A} + \mathbf{B})^{-1*} (\mathbf{A} + \mathbf{A}^*) (\mathbf{A} + \mathbf{B})^{-1} (\mathbf{B} + \mathbf{B}^*) \tag{16}$$

and

$$\mathbf{L} = (\mathbf{A} + \mathbf{B})^{-1*} (\mathbf{B} + \mathbf{B}^*) (\mathbf{A} + \mathbf{B})^{-1} (\mathbf{A} + \mathbf{A}^*) \,. \tag{17}$$

Then $\mathbf{K}$ and $\mathbf{L}$ have the same eigenvalues, counting multiplicities (i.e., they have the same characteristic polynomial).

Proof: See Appendix B □

Let $\mathbf{A}$ be a positive semidefinite matrix. We know that [18, Sec. 7.2.6] there exists a unique positive semidefinite matrix $\mathbf{B}$ such that $\mathbf{B}^2 = \mathbf{A}$. The matrix $\mathbf{B}$ is referred to as the unique positive semidefinite square root of $\mathbf{A}$, and is denoted by $\mathbf{A}^{1/2}$. If $\mathbf{A}$ is invertible, we may write $\mathbf{A}^{-1/2} = (\mathbf{A}^{1/2})^{-1} = (\mathbf{A}^{-1})^{1/2}$. Since $H(\mathbf{Y}_{GA})$ and $H(\mathbf{Y}_{GB})$ are positive definite, we can define the matrices

$$\begin{aligned} \mathbf{M}_1 = {} & (\mathbf{Y}_{GA} + \mathbf{Y}_{GA}^*)^{1/2} \, \mathbf{Z}_{PAB}^* \\ & \times (\mathbf{Y}_{GB} + \mathbf{Y}_{GB}^*) \mathbf{Z}_{PAB} (\mathbf{Y}_{GA} + \mathbf{Y}_{GA}^*)^{1/2} \,, \end{aligned} \tag{18}$$

and

$$\begin{aligned} \mathbf{M}_2 = {} & (\mathbf{Y}_{GB} + \mathbf{Y}_{GB}^*)^{1/2} \, \mathbf{Z}_{PAB}^* \\ & \times (\mathbf{Y}_{GA} + \mathbf{Y}_{GA}^*) \mathbf{Z}_{PAB} (\mathbf{Y}_{GB} + \mathbf{Y}_{GB}^*)^{1/2} \,, \end{aligned} \tag{19}$$

which are both of size N by N. $\mathbf{M}_1$ and $\mathbf{M}_2$ are clearly hermitian, so that their eigenvalues are real. Note that the eigenvalues of $\mathbf{M}_1$ and $\mathbf{M}_2$ are dimensionless numbers, since $\mathbf{M}_1$ and $\mathbf{M}_2$ are dimensionless matrices.

Theorem 7. The matrices $\mathbf{M}_1$ and $\mathbf{M}_2$ defined by (18) and (19) are positive semidefinite, so that their eigenvalues are nonnegative. Let $\lambda_{1\max}$ be the largest eigenvalue of $\mathbf{M}_1$ and $\lambda_{1\min}$ the smallest eigenvalue of $\mathbf{M}_1$. Let $\lambda_{2\max}$ be the largest eigenvalue of $\mathbf{M}_2$ and $\lambda_{2\min}$ the smallest eigenvalue of $\mathbf{M}_2$. We have

$$0 \leqslant \lambda_{1\min} \leqslant \lambda_{1\max} \leqslant 1 \,, \tag{20}$$

$$0 \leqslant \lambda_{2\min} \leqslant \lambda_{2\max} \leqslant 1 \,, \tag{21}$$

$$0 \leqslant \lambda_{1\min} P_{AAVG} \leqslant P_{ADG} \leqslant \lambda_{1\max} P_{AAVG}\,, \quad (22)$$

and

$$0 \leqslant \lambda_{2\min} P_{BAVG} \leqslant P_{BDG} \leqslant \lambda_{2\max} P_{BAVG}\,. \quad (23)$$

Moreover,

- the equality $P_{ADG} = \lambda_{1\max} P_{AAVG}$ is satisfied if $\mathbf{I}_{SGA}$ is the product of $(\mathbf{Y}_{GA} + \mathbf{Y}^*_{GA})^{1/2}$ and an eigenvector of $\mathbf{M}_1$ associated with $\lambda_{1\max}$, measured in $\mathrm{A}^{1/2}\mathrm{V}^{1/2}$;
- the equality $P_{ADG} = \lambda_{1\min} P_{AAVG}$ is satisfied if $\mathbf{I}_{SGA}$ is the product of $(\mathbf{Y}_{GA} + \mathbf{Y}^*_{GA})^{1/2}$ and an eigenvector of $\mathbf{M}_1$ associated with $\lambda_{1\min}$, measured in $\mathrm{A}^{1/2}\mathrm{V}^{1/2}$;
- the equality $P_{BDG} = \lambda_{2\max} P_{BAVG}$ is satisfied if $\mathbf{I}_{SGB}$ is the product of $(\mathbf{Y}_{GB} + \mathbf{Y}^*_{GB})^{1/2}$ and an eigenvector of $\mathbf{M}_2$ associated with $\lambda_{2\max}$, measured in $\mathrm{A}^{1/2}\mathrm{V}^{1/2}$; and
- the equality $P_{BDG} = \lambda_{2\min} P_{BAVG}$ is satisfied if $\mathbf{I}_{SGB}$ is the product of $(\mathbf{Y}_{GB} + \mathbf{Y}^*_{GB})^{1/2}$ and an eigenvector of $\mathbf{M}_2$ associated with $\lambda_{2\min}$, measured in $\mathrm{A}^{1/2}\mathrm{V}^{1/2}$.

Moreover, $\mathbf{M}_1$ and $\mathbf{M}_2$ have the same characteristic polynomial, so that $\lambda_{1\max} = \lambda_{2\max}$ and $\lambda_{1\min} = \lambda_{2\min}$.

Proof: $H(\mathbf{Y}_{GB})$ being positive definite, $\mathbf{M}_1$ is positive semidefinite by [18, Sec. 7.1.8], so that its eigenvalues are nonnegative by [18, Sec. 7.1.4]. For CA, let us introduce the new variable $\mathbf{X}_1 = (\mathbf{Y}_{GA}+\mathbf{Y}^*_{GA})^{-1/2}\,\mathbf{I}_{SGA}$. Since $\mathbf{I}_{SGA} = (\mathbf{Y}_{GA} + \mathbf{Y}^*_{GA})^{1/2}\,\mathbf{X}_1$, it follows from (5), (11) and (18) that

$$P_{AAVG} = \frac{1}{2}\mathbf{X}_1^*\mathbf{X}_1 \quad \text{and} \quad P_{ADG} = \frac{1}{2}\mathbf{X}_1^*\mathbf{M}_1\mathbf{X}_1\,. \quad (24)$$

By Rayleigh's theorem [18, Sec. 4.2.2], we have

$$0 \leqslant \lambda_{1\min}\mathbf{X}_1^*\mathbf{X}_1 \leqslant \mathbf{X}_1^*\mathbf{M}_1\mathbf{X}_1 \leqslant \lambda_{1\max}\mathbf{X}_1^*\mathbf{X}_1\,, \quad (25)$$

which, used with (24), proves (22). The other assertions of Theorem 1 relating to $\mathbf{M}_1$ also result from Rayleigh's theorem and the definition of $\mathbf{X}_1$. The fact that $\lambda_{1\max} \leqslant 1$ is a consequence of the fact that there exists a value of $\mathbf{X}_1$ for which $P_{ADG} = \lambda_{1\max} P_{AAVG}$, while the definition of the available power entails $P_{ADG} \leqslant P_{AAVG}$. The arguments for the assertions of Theorem 1 relating to $\mathbf{M}_2$ and for $\lambda_{2\max} \leqslant 1$ are similar.

Since $(\mathbf{Y}_{GA} + \mathbf{Y}^*_{GA})^{1/2}$ and $(\mathbf{Y}_{GB} + \mathbf{Y}^*_{GB})^{1/2}$ are invertible square matrices, it follows from [18, Sec. 1.3.22] that $\mathbf{M}_1$ has the same eigenvalues, counting multiplicities, as

$$\mathbf{N}_1 = \mathbf{Z}^*_{PAB}(\mathbf{Y}_{GB} + \mathbf{Y}^*_{GB})\mathbf{Z}_{PAB}(\mathbf{Y}_{GA} + \mathbf{Y}^*_{GA})\,, \quad (26)$$

and that $\mathbf{M}_2$ has the same eigenvalues, counting multiplicities, as

$$\mathbf{N}_2 = \mathbf{Z}^*_{PAB}(\mathbf{Y}_{GA} + \mathbf{Y}^*_{GA})\mathbf{Z}_{PAB}(\mathbf{Y}_{GB} + \mathbf{Y}^*_{GB})\,, \quad (27)$$

Applying Lemma 3 to $\mathbf{Y}_{GA}$ and $\mathbf{Y}_{GB}$, and using (13), we find that $\mathbf{N}_1$ and $\mathbf{N}_2$ have the same characteristic polynomial, so that $\mathbf{M}_1$ and $\mathbf{M}_2$ have the same characteristic polynomial. Thus, $\lambda_{1\max} = \lambda_{2\max}$ and $\lambda_{1\min} = \lambda_{2\min}$. □

Observation 5. We note that, if we only need the eigenvalues of $\mathbf{M}_1$ or $\mathbf{M}_2$, the shortest computation is a direct computation of the eigenvalues of $\mathbf{N}_1$ or $\mathbf{N}_2$ defined by (26) and (27).

Using Theorem 7, we get the new *Reciprocal theorem on the power transfer ratios*, which reads as follows.

Theorem 8. Ignoring noise power contributions, we assert that:

(a) the set of the values of the power transfer ratio t_A, obtained for all nonzero $\mathbf{V}_{OGA} \in \mathbb{C}^N$, or equivalently for all nonzero $\mathbf{I}_{SGA} \in \mathbb{C}^N$, has a least element referred to as "minimum value", and a greatest element referred to as "maximum value";

(b) the set of the values of the power transfer ratio t_B, obtained for all nonzero $\mathbf{V}_{OGB} \in \mathbb{C}^N$, or equivalently for all nonzero $\mathbf{I}_{SGB} \in \mathbb{C}^N$, has a least element referred to as "minimum value", and a greatest element referred to as "maximum value";

(c) the maximum value of t_A and the maximum value of t_B are equal to $\lambda_{1\max} = \lambda_{2\max}$; and

(d) the minimum value of t_A and the minimum value of t_B are equal to $\lambda_{1\min} = \lambda_{2\min}$.

The reciprocal theorem on the power transfer ratios extends (1) to multiport generators and multiport loads, in the sense that it creates a relationship between t_A and t_B.

IV. SUPPLEMENT, EXAMPLE AND COMMENTS

A. USE OF AN EXTREMUM-SEEKING ALGORITHM

An extremum-seeking algorithm can be used to approximate the maximum and minimum values defined in (a) and (b) of Theorem 8, instead of computing them as eigenvalues according to Theorem 7.

It follows from (14) that the power transfer ratio t_A is not modified if $\mathbf{I}_{SGA}$ is multiplied by an arbitrary nonzero complex number. Thus, to approximate the maximum and minimum values of t_A, an extremum-seeking algorithm may posit $\mathbf{I}_{SGA} \in \mathbb{S}_N$, and further assume that one of the entries of $\mathbf{I}_{SGA}$ is real and nonnegative. By the same token, it follows from (15) that, to approximate the maximum and minimum values of t_B, an extremum-seeking algorithm may posit $\mathbf{I}_{SGB} \in \mathbb{S}_N$, and further assume that one of the entries of $\mathbf{I}_{SGB}$ is real and nonnegative. These observations lead to the simple parametrizations already used in Section VI of Part 1. For instance, for $N = 2$, the numerical algorithm can use

$$\mathbf{I}_{SGA} = \begin{pmatrix} \sin\theta_1 \exp j\phi_1 \\ \cos\theta_1 \end{pmatrix} \quad (28)$$

in CA, where $\theta_1 \in [0, \pi/2]$ and $\phi_1 \in [-\pi, \pi]$, and

$$\mathbf{I}_{SGB} = \begin{pmatrix} \sin\theta_2 \exp j\phi_2 \\ \cos\theta_2 \end{pmatrix} \quad (29)$$

in CB, where $\theta_2 \in [0, \pi/2]$ and $\phi_2 \in [-\pi, \pi]$. Thus, for $N = 2$, to estimate each maximum or minimum value defined in (a) and (b) of Theorem 8, an extremum-seeking algorithm may solve a problem having only 2 real unknowns each lying in a bounded interval.

B. EXAMPLE

As an example, let us assume that

$$\mathbf{Z}_{GA} = \begin{pmatrix} 51+39j & 19+79j \\ 27+56j & 37+61j \end{pmatrix} \Omega\,, \tag{30}$$

and

$$\mathbf{Z}_{GB} = \begin{pmatrix} 32+87j & 11+41j \\ 23+37j & 73+13j \end{pmatrix} \Omega\,. \tag{31}$$

$\mathbf{Z}_{GA}$ and $\mathbf{Z}_{GB}$ are not symmetric and have each a positive definite hermitian part. The maximum and minimum values defined in (a) and (b) of Theorem 8 have been computed as eigenvalues according to Theorem 7, and independently determined by an extremum-seeking algorithm using (28) or (29). Both methods give exactly the same values, shown in Table 1.

TABLE 1. Results for the example.

Quantity	CA	CB
maximum value of the power transfer ratio	0.864763	0.864763
minimum value of the power transfer ratio	0.215189	0.215189

Thus, $\mathbf{Z}_{GA}$ and $\mathbf{Z}_{GB}$ being not symmetric, we find that the power transfer ratio equalities stated in (c) and (d) of Theorem 8 are compatible with the computed values.

C. ON THE PROOF OF THEOREM 7

To prove Theorem 7 except its last assertion, we could have utilized Theorem 3, which was stated and proven in Part 1.

To this end, we decide that the DUS considered in Part 1 is such that $n = m = N$, and consists only of wires which, for any integer $p \in \{1, \ldots, m\}$, directly connect port p of port set 1 of the DUS to port p of port set 2 of the DUS (positive terminal to positive terminal and negative terminal to negative terminal). We can of course consider that this DUS is present in Fig. 2, port set 1 of the DUS being connected to the "N-port generator (in CA) or load (in CB)", and port set 2 of the DUS being connected to the "N-port load (in CA) or generator (in CB)". This DUS has neither an impedance matrix nor an admittance matrix. By Theorem 1 (stated in Part 1), the parallel-augmented multiport comprising this DUS and defined in Section IV of Part 1 has an impedance matrix $\mathbf{Z}_{PAM}$, which is given by

$$\mathbf{Z}_{PAM} = \begin{pmatrix} \mathbf{Z}_{PAM11} & \mathbf{Z}_{PAM12} \\ \mathbf{Z}_{PAM21} & \mathbf{Z}_{PAM22} \end{pmatrix} \tag{32}$$

in block form, where $\mathbf{Z}_{PAM11} = \mathbf{Z}_{PAM12} = \mathbf{Z}_{PAM21} = \mathbf{Z}_{PAM22} = \mathbf{Z}_{PAB}$. Since, using the notations of Section III of Part 1, we have $\mathbf{Z}_{S1} = \mathbf{Z}_{GA}$ and $\mathbf{Z}_{S2} = \mathbf{Z}_{GB}$, it follows that (18) and (19) exactly correspond to equations (19) and (20) of Part 1. This shows that Theorem 7, except its last assertion, can be derived from Theorem 3.

If we introduce the additional assumption that $\mathbf{Z}_{GA}$ and $\mathbf{Z}_{GB}$ are symmetric, then $\mathbf{Z}_{PAB}$ is symmetric because the inverse of an invertible symmetric matrix is symmetric. In this case, the last assertion of Theorem 7 (that is, $\lambda_{1\max} = \lambda_{2\max}$ and $\lambda_{1\min} = \lambda_{2\min}$) can also be derived from Theorem 3, so that Theorem 7 is only a corollary of Theorem 3. However, if we remove this unnecessary assumption, Theorem 3 says nothing about this last assertion of Theorem 7, and Section VI.B of Part 1 shows that this limitation is inherent to Theorem 3. It is interesting to note that the matrices used in the example of Section IV.B above are also used in the example of Section VI.B of Part 1.

We can say that the proof of Theorem 7 provided in Section III, which is based on Lemma 3, was needed to remove an unnecessary assumption, the symmetry of $\mathbf{Z}_{GA}$ and $\mathbf{Z}_{GB}$.

D. ON THE PREMISES OF THEOREM 7 AND THEOREM 8

The only assumption of Theorem 7 and Theorem 8 is: $\mathbf{Z}_{GA}$ and $\mathbf{Z}_{GB}$ exist and are such that $H(\mathbf{Z}_{GA})$ and $H(\mathbf{Z}_{GB})$ are positive definite (or, equivalently: $\mathbf{Y}_{GA}$ and $\mathbf{Y}_{GB}$ exist and are such that $H(\mathbf{Y}_{GA})$ and $H(\mathbf{Y}_{GB})$ are positive definite). As said in Section II, this assumption ensures that P_{AAVG} and P_{BAVG} are defined. However, if $N \geqslant 2$, it is possible to design theoretical N-port generators for which an available power can be defined, but which do not satisfy this assumption. For instance, for $N = 2$, such a theoretical N-port generator may comprise a single-port generator having an internal impedance of $1.0\,\Omega$, this single-port generator being directly connected to ports 1 and 2 of the N-port generator (positive terminal to positive terminal and negative terminal to negative terminal).

V. POWER MATCH FIGURE AND RETURN FIGURE

A. THE POWER MATCH FIGURE

Let us assume that $\mathbf{Y}_{GA}$ and $\mathbf{Y}_{GB}$ are known. If $\mathbf{I}_{SGA}/||\mathbf{I}_{SGA}||_2$ and $\mathbf{I}_{SGB}/||\mathbf{I}_{SGB}||_2$ are constant and known, we can compute t_A and t_B using (14) and (15). In the opposite case, we need a suitable metric of the power transfer ratios. To obtain such a suitable metric, we consider the worst-case situation, that is the lowest power transfer. Using Theorem 8, let $t_{MIN} = \lambda_{1\min} = \lambda_{2\min}$ be the minimum value of t_A, which is equal to the minimum value of t_B. The power match figure is F_M defined by

$$F_M = \sqrt{1 - t_{MIN}}\,, \tag{33}$$

Using (7) and (20), or (8) and (21), we get

$$0 \leqslant F_M \leqslant 1\,. \tag{34}$$

F_M expressed in decibels is $F_{MdB} = 20 \log F_M$. By Theorem 1, $F_M = 0$ means that:

- for any excitation in CA, we have $t_A = 1$ or equivalently $P_{ADG} = P_{AAVG}$; and
- for any excitation in CB, we have $t_B = 1$ or equivalently $P_{BDG} = P_{BAVG}$.

In fact, $F_M = 0$ entails $\lambda_{1\min} = \lambda_{1\max} = \lambda_{2\min} = \lambda_{2\max} = 1$, so that $\mathbf{M}_1 = \mathbf{M}_2 = \mathbf{1}_N$, where $\mathbf{1}_N$ is the identity matrix of size N by N, because $\mathbf{M}_1$ and $\mathbf{M}_2$ being hermitian, they are diagonalizable.

$F_M = 1$ does not lead to a result applicable to an arbitrary excitation, since it means that:

- in CA, there exists at least one nonzero $\mathbf{V}_{OGA}$ or nonzero $\mathbf{I}_{SGA}$ such that $t_A = 0$ or equivalently $P_{ADG} = 0$; and
- in CB, there exists at least one nonzero $\mathbf{V}_{OGB}$ or nonzero $\mathbf{I}_{SGB}$ such that $t_B = 0$ or equivalently $P_{BDG} = 0$.

The use of F_M as a design parameter is relevant to situations in which the location of $\mathbf{I}_{SGA}/||\mathbf{I}_{SGA}||_2$ on $\mathbb{S}_N$ is not constant or is not known, or in which the location of $\mathbf{I}_{SGB}/||\mathbf{I}_{SGB}||_2$ on $\mathbb{S}_N$ is not constant or is not known.

B. THE RETURN FIGURE

Let r_0 be a positive arbitrary reference resistance used to define: a scattering matrix $\mathbf{S} = [S_{pq}]$ of the N-port load used in CA, at f_G; a vector of the rms normalized incident voltage waves in CA, denoted by $\mathbf{a}$; and the resulting vector of the rms normalized reflected voltage waves in CA, denoted by $\mathbf{b}$ and given by $\mathbf{b} = \mathbf{S}\mathbf{a}$. Since r_0 is real, $\mathbf{a}^*\mathbf{a} = ||\mathbf{a}||_2^2$ is the incident power seen by the N ports of the N-port load used in CA (for the arbitrary r_0), and $\mathbf{b}^*\mathbf{b} = ||\mathbf{b}||_2^2$ is the reflected power (for the arbitrary r_0) [20, Ch. 24]. We may want to minimize the ratio $r(\mathbf{a})$ defined, for any $\mathbf{a} \neq \mathbf{0}$, by

$$r(\mathbf{a}) = \frac{||\mathbf{b}||_2}{||\mathbf{a}||_2} = \sqrt{\frac{\mathbf{b}^*\mathbf{b}}{\mathbf{a}^*\mathbf{a}}} \,. \tag{35}$$

For a fixed $\mathbf{a}/||\mathbf{a}||_2$, we see that $r(\mathbf{a})$ does not depend on $||\mathbf{a}||_2$. Following [18, Section 8.1], we define $|\mathbf{S}| = [|S_{pq}|]$. This entrywise absolute value of $\mathbf{S}$ is a nonnegative matrix. An integer $q \in \{1, \ldots, N\}$ being chosen, the knowledge of $|S_{pq}|$ for every $p \in \{1, \ldots, N\}$ allows us to directly compute $r(\mathbf{a})$ if only port q is excited, that is, if only the q-th entry of $\mathbf{a}$ is nonzero. Thus, the knowledge of $|\mathbf{S}|$ allows us to directly compute $r(\mathbf{a})$ for the N possible single-port excitations, but not what happens when several entries of $\mathbf{a}$ are nonzero.

If the location of $\mathbf{a}/||\mathbf{a}||_2$ on $\mathbb{S}_N$ is not constant or not known, a relevant metric for reflected waves is the worst possible value of $r(\mathbf{a})$, which is the return figure F_R defined in [7]–[11] as:

$$F_R = |||\mathbf{S}|||_2 = \max_{\mathbf{a}\neq\mathbf{0}} \frac{||\mathbf{b}||_2}{||\mathbf{a}||_2} = \max_{\mathbf{a}\neq\mathbf{0}} r(\mathbf{a}) \,, \tag{36}$$

where $|||\mathbf{M}|||_2$ denotes the spectral norm of a square matrix $\mathbf{M}$, and where we have used the fact that the spectral norm is the matrix norm induced by the euclidian norm on vectors [18, Section 5.6.6]. $|||\mathbf{S}|||_2$ is the greatest singular value of $\mathbf{S}$, which is the square root of the greatest eigenvalue of $\mathbf{S}^*\mathbf{S}$, and also the square root of the greatest eigenvalue of $\mathbf{S}\mathbf{S}^*$ by [18, Section 1.3.22].

The N-port load used in CA being assumed passive, we have

$$0 \leqslant F_R \leqslant 1 \,, \tag{37}$$

since, for any $\mathbf{a}$, we have $0 \leqslant r(\mathbf{a}) \leqslant 1$. We observe that F_R^2 is the maximum value of the ratio of the reflected power to the incident power for all nonzero excitations, because

$$F_R^2 = \left(\max_{\mathbf{a}\neq\mathbf{0}} \sqrt{\frac{\mathbf{b}^*\mathbf{b}}{\mathbf{a}^*\mathbf{a}}} \right)^2 = \max_{\mathbf{a}\neq\mathbf{0}} \frac{\mathbf{b}^*\mathbf{b}}{\mathbf{a}^*\mathbf{a}} \,, \tag{38}$$

F_R expressed in decibels is $F_{RdB} = 20 \log F_R$. It follows from (38) that, for the reference resistance r_0, F_{RdB} is the greatest value of the ratio, expressed in decibels, of the reflected power to the incident power, for all nonzero excitations. We can say that, with respect to the reference resistance r_0, the N-port load used in CA is exactly decoupled and matched for any nonzero excitation if and only if $F_R = 0$ or $F_{RdB} = -\infty$ dB.

It is well known that we always have [20, Ch. 24]:

$$P_{ADG} = \mathbf{a}^*\mathbf{a} - \mathbf{b}^*\mathbf{b} \,. \tag{39}$$

Let us assume that $\mathbf{Z}_{GA} = r_0 \mathbf{1}_N$. This means that the ports of the N-port generator used in CA, or of the N-port load used in CB, are uncoupled and present the same real impedance r_0. In this case,

$$P_{AAVG} = \frac{1}{4r_0} \mathbf{V}_{OGA}^* \mathbf{V}_{OGA} = \mathbf{a}^*\mathbf{a} \,, \tag{40}$$

in which we have used (3). In this case, using (7), (35), (39) and (40), we find that

$$t_A = \frac{\mathbf{a}^*\mathbf{a} - \mathbf{b}^*\mathbf{b}}{\mathbf{a}^*\mathbf{a}} = 1 - r(\mathbf{a})^2 \,. \tag{41}$$

Using (33) and the fact that a maximum value of $r(\mathbf{a})$ corresponds to a minimum value of t_A, we may conclude that $\mathbf{Z}_{GA} = r_0 \mathbf{1}_N$ entails

$$F_R = F_M \,, \tag{42}$$

so that the return figure is related to the minimum values of the return ratios t_A and t_B, by (33).

C. MATCHING METRICS FOR N-PORTS

F_M and F_R are instances of a matching metric, where "matching metric" refers to one of more real quantities representing how $\mathbf{Z}_{GB}$ is harmonized with a wanted impedance matrix $\mathbf{Z}_W$.

As said above, $F_M = 0$ if and only if, for any excitation in CA, we have $P_{ADG} = P_{AAVG}$, corresponding to a maximum power transfer. According to the maximum power transfer theorem [19], the ideal value $F_M = 0$ occurs if and only if $\mathbf{Z}_{GB} = \mathbf{Z}_{GA}^*$. Thus, in the case of the metric F_M, we have $\mathbf{Z}_W = \mathbf{Z}_{GA}^*$. This metric has a profound meaning since, according to (33), we have

$$\min_{\mathbf{I}_{\mathbf{SGA}}\neq\mathbf{0}} t_A = \min_{\mathbf{I}_{\mathbf{SGB}}\neq\mathbf{0}} t_B = 1 - F_M^2 \,. \tag{43}$$

$F_R = 0$ being equivalent to $\mathbf{b} = \mathbf{0}$, the ideal value $F_R = 0$ occurs if and only if $\mathbf{Z}_{GB} = r_0 \mathbf{1}_N$ or equivalently $\mathbf{S} = \mathbf{0}$. Thus, in the case of the metric F_R, we have $\mathbf{Z}_W = r_0 \mathbf{1}_N$. By (42), this metric inherits the properties of F_M if $\mathbf{Z}_{GA} = r_0 \mathbf{1}_N$. However, unlike F_M, F_R is defined in the more general case in which the device connected to the N-port load used in CA is not LTI.

The most popular matching metric is the entries of $|\mathbf{S}|$. This metric also corresponds to $\mathbf{Z}_W = r_0 \mathbf{1}_N$ because the ideal value $|\mathbf{S}| = \mathbf{0}$ occurs if and only if $\mathbf{Z}_{GB} = r_0 \mathbf{1}_N$. Unlike F_M and F_R, $|\mathbf{S}|$ is not a scalar, so that it is not suitable to compare two arbitrary N-ports. The connection between $|\mathbf{S}|$ and F_R will be thoroughly discussed in Section VI.

D. THE POWER MATCH FIGURE AS A MATRIX NORM

The return figure F_R was defined as a matrix norm in (36), but we have used a different approach to define the power match figure F_M in (33). We want to find out if F_M is also a matrix norm.

If $\mathbf{u} \in \mathbb{C}^N$ is an eigenvector of $\mathbf{M}_1$ associated with the eigenvalue λ, it follows from Theorem 7 that $\lambda \in [0, 1]$, so that $\mathbf{u}$ is an eigenvector of $\mathbf{1}_N - \mathbf{M}_1$ associated with the eigenvalue $1 - \lambda$, which lies in $[0, 1]$. Since $\mathbf{1}_N - \mathbf{M}_1$ is an hermitian matrix, it follows that it is positive semidefinite, so that $(\mathbf{1}_N - \mathbf{M}_1)^{1/2}$ is defined. Likewise, if $\mathbf{u} \in \mathbb{C}^N$ is an eigenvector of $\mathbf{M}_2$ associated with the eigenvalue λ, then $(\mathbf{1}_N - \mathbf{M}_2)^{1/2}$ is defined.

$(\mathbf{1}_N - \mathbf{M}_1)^{1/2}$ being positive semidefinite, its spectral norm $|||(\mathbf{1}_N - \mathbf{M}_1)^{1/2}|||_2$ is the square root of the greatest eigenvalue of $\mathbf{1}_N - \mathbf{M}_1$, this square root being equal to $\sqrt{1 - t_{MIN}}$. Likewise, $(\mathbf{1}_N - \mathbf{M}_2)^{1/2}$ being positive semidefinite, its spectral norm is equal to $\sqrt{1 - t_{MIN}}$.

Thus, it follows from (33) that

$$F_M = |||(\mathbf{1}_N - \mathbf{M}_1)^{1/2}|||_2 = |||(\mathbf{1}_N - \mathbf{M}_2)^{1/2}|||_2 \,. \quad (44)$$

It follows from (44) that F_M is a matrix norm and an induced norm, though (44) is not advisable for an actual computation of F_M. However, our derivation also shows that

$$F_M = \sqrt{\rho(\mathbf{1}_N - \mathbf{M}_1)} = \sqrt{\rho(\mathbf{1}_N - \mathbf{M}_2)} \,, \quad (45)$$

where $\rho(\mathbf{M})$ denotes the spectral radius of an arbitrary square matrix $\mathbf{M}$, that is the largest absolute value of its eigenvalues. For an actual computation of F_M, (45) and (33) are equally convenient.

VI. MORE PROPERTIES OF THE RETURN FIGURE

We now want to study the relationships between $|\mathbf{S}|$ and the return figure F_R. Let us first consider three examples. In example 1, we have

$$\mathbf{S} = \begin{pmatrix} 0.50 & 0.25 \\ 0.25 & 0.50 \end{pmatrix} , \quad (46)$$

for which $F_R = 0.750$ and $F_{RdB} \simeq -2.499$ dB. In example 2, we have

$$\mathbf{S} = \begin{pmatrix} 0.50 & 0.25j \\ 0.25j & 0.50 \end{pmatrix} , \quad (47)$$

for which $F_R \simeq 0.559$ and $F_{RdB} \simeq -5.052$ dB. In example 3, we have

$$\mathbf{S} = \begin{pmatrix} 0.50 & 0.25 \\ 0.25 & 0.50j \end{pmatrix} , \quad (48)$$

for which $F_R \simeq 0.699$ and $F_{RdB} \simeq -3.104$ dB. Since (46)-(48) correspond to the same $|\mathbf{S}|$, we have proved that F_R cannot be derived from the sole knowledge of $|\mathbf{S}|$.

To explore how $|\mathbf{S}|$ can be utilized to obtain useful upper bounds on F_R, we can introduce $\mathbf{A} = [A_{pq}] = \mathbf{S}^*\mathbf{S}$ and $\mathbf{B} = [B_{pq}] = |\mathbf{S}|^T|\mathbf{S}|$, where the superscript T denotes the transpose. For any p and q lying in $\{1, \ldots, N\}$, we have

$$|A_{pq}| = \left| \sum_{k=1}^{N} \bar{S}_{kp} S_{kq} \right| \leqslant \sum_{k=1}^{N} |S_{kp}|\,|S_{kq}| = B_{pq} \quad (49)$$

and

$$A_{pp} = \sum_{k=1}^{N} |S_{kp}|^2 = B_{pp} \,. \quad (50)$$

Let $\mathbf{M} = [M_{pq}]$ be a complex matrix of size N by N. By [18, Section 5.6.P23], we have

$$|||\mathbf{M}|||_2 \leqslant ||\mathbf{M}||_2 \leqslant \sqrt{N}\; |||\mathbf{M}|||_2 \,, \quad (51)$$

where

$$||\mathbf{M}||_2 = \sqrt{\sum_{p=1}^{N} \sum_{q=1}^{N} |M_{pq}|^2} \quad (52)$$

is the Frobenius norm of the matrix $\mathbf{M}$. It follows from (36), (50) and (51) that we can define m_E such that

$$F_R \leqslant m_E = ||\mathbf{S}||_2 = \sqrt{\mathrm{tr}(\mathbf{B})} \,. \quad (53)$$

Thus, m_E is an upper bound on F_R, and such that m_E is only determined by $\mathbf{B}$, and therefore only determined by $|\mathbf{S}|$. It follows from (37) that (53) is useful only if $m_E < 1$.

It follows from (36) that $F_R^2 = \rho(\mathbf{A})$. The theory of Geršgorin disks allows us to write

$$\rho(\mathbf{A}) \leqslant \max_p \sum_{q=1}^{N} |A_{pq}| = \max_q \sum_{p=1}^{N} |A_{pq}| \,, \quad (54)$$

where we have used the fact that $\mathbf{A}$ is hermitian and [18, Section 6.1.5]. Using (49) and (54), we find that we can define m_G such that

$$F_R \leqslant m_G = \sqrt{\max_p \sum_{q=1}^{N} B_{pq}} \,. \quad (55)$$

This information on F_R is only derived from $|\mathbf{S}|$. It follows from (37) that (55) is useful only if $m_G < 1$.

It is possible to obtain an upper bound which is only based on $|\mathbf{S}|$, and closer to F_R than m_E and m_G. Using the fact that $\mathbf{A}$ is hermitian, (49) and Fan's theorem [18, Section 8.2.9], we obtain

$$\rho(\mathbf{A}) \in \bigcup_{q=1}^{N} \{x \in \mathbb{R} : |x - A_{qq}| \leqslant \rho(\mathbf{B}) - B_{qq}\} \,, \quad (56)$$

where the colon means "such that". Using (50), we get

$$\rho(\mathbf{A}) \in \bigcup_{q=1}^{N} \{x \in \mathbb{R} : -\rho(\mathbf{B}) + 2A_{qq} \leqslant x \leqslant \rho(\mathbf{B})\} \,. \quad (57)$$

Thus, $\rho(\mathbf{A}) \leqslant \rho(\mathbf{B})$ and we can define m_F such that

$$F_R \leqslant m_F = \sqrt{\rho(\mathbf{B})} \,. \quad (58)$$

If we know $|\mathbf{S}|$ and do not make any other assumption, it is possible that $\mathbf{S} = |\mathbf{S}|$, in which case $\mathbf{A} = \mathbf{B}$ and $F_R = m_F$. It follows that m_F is the least (and the best) of all upper bounds on F_R which are only based on $|\mathbf{S}|$. Thus, the upper bounds m_E, m_G and m_F on F_R are only based on $|\mathbf{S}|$ and satisfy

$$m_F \leqslant m_G \;\text{ and }\; m_F \leqslant m_E \,. \quad (59)$$

It follows from (37) that (58) is useful only if $\rho(\mathbf{B}) < 1$.

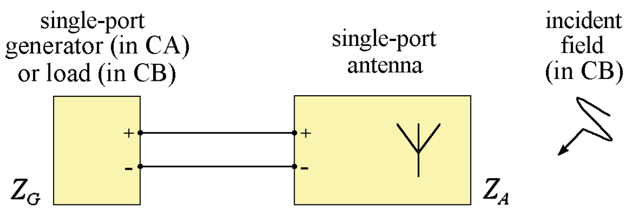

FIGURE 3. The two configurations, CA and CB, considered in Section VII.A for a single antenna.

In examples 1 to 3 defined above, (53) gives $F_R \leqslant m_E \simeq 0.791$, whereas (55) and (58) give $F_R \leqslant m_F = m_G = 0.750$, which may be compared to $F_R = 0.750$ in example 1, $F_R \simeq 0.559$ in example 2 and $F_R \simeq 0.699$ in example 3. To prove that (55) and (58) do not always give the same result, we may consider the two following examples. In example 4, we have

$$\mathbf{S} = \begin{pmatrix} 0.50 & 0.25 \\ 0.25 & 0.40 \end{pmatrix}, \tag{60}$$

for which $F_R \simeq 0.705$. In example 5, we have

$$\mathbf{S} = \begin{pmatrix} 0.50 & 0.25j \\ 0.25j & 0.40 \end{pmatrix}, \tag{61}$$

for which $F_R \simeq 0.565$. For examples 4 and 5, (53) gives $F_R \leqslant m_E \simeq 0.731$, (55) gives $F_R \leqslant m_G \simeq 0.733$ and (58) gives $F_R \leqslant m_F \simeq 0.705$.

In this Section VI, we have: shown that $|\mathbf{S}|$ does not determine F_R; computed three upper bounds m_E, m_G and m_F on F_R, these upper bounds being solely derived from the knowledge of $|\mathbf{S}|$; shown that these upper bounds are distinct; and shown that m_F is the least of all possible upper bounds solely derived from the knowledge of $|\mathbf{S}|$. These results clarify the relationship between $|\mathbf{S}|$ and F_R.

VII. APPLICATION TO A MAA

A. GENERAL CONSIDERATIONS

Fig. 3 shows two configurations in which the device drawn on the right in Fig. 1 is an LTI passive antenna operating in the harmonic steady state, at a given frequency. Here, "passive antenna" is used in the meaning of antenna engineering, the passive antenna, if regarded as a single-port circuit element of circuit theory, being passive in the context of emission, but active in the context of reception. Let Z_A denote the impedance of the antenna. In configuration A (CA) used for emission, the port of the antenna is connected to an LTI generator of internal impedance Z_G, and there is no incident field. In configuration B (CB) used for reception, the port of the antenna is connected to an LTI load of impedance Z_G, and the antenna is excited by an incident field. Let us use:

- P_{AAVG} to denote the average power available from the generator, in CA (emission);
- P_{ARPA} to denote the average power received by the port of the antenna, in CA (emission);
- P_{BAVA} to denote the average power available from the port of the antenna, in CB (reception); and
- P_{BDPA} to denote the average power delivered by the port of the antenna, in CB (reception).

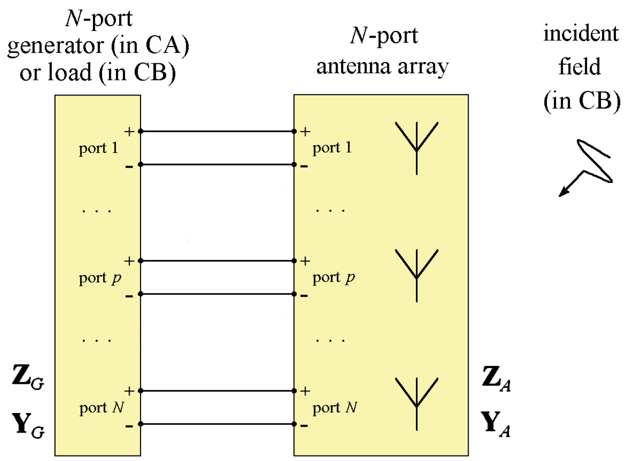

FIGURE 4. The two configurations, CA and CB, considered in Section VII.A for a multiport antenna array (MAA).

What was said in Section I is directly applicable to the configurations shown in Fig. 3, if we use $Z_G = Z_{GA}$; $Z_A = Z_{GB}$; $P_{ARPA} = P_{ADG}$; $P_{BAVA} = P_{BAVG}$ and $P_{BDPA} = P_{BDG}$. It follows that $t_A = P_{ARPA}/P_{AAVG}$ and $t_B = P_{BDPA}/P_{BAVA}$.

Fig. 4 shows two configurations in which the device drawn on the right in Fig. 2 is an LTI and passive multiport antenna array (MAA), where "passive" is again used in the meaning of antenna engineering. The MAA has N ports, and is operating in the harmonic steady state, at the given frequency f_G. The MAA has an impedance matrix $\mathbf{Z}_A$ at f_G. In configuration A (CA) used for emission, the MAA is connected to an LTI N-port generator of internal impedance matrix $\mathbf{Z}_G$ at f_G, and there is no incident field. In configuration B (CB) used for reception, the MAA is connected to an LTI N-port load of impedance matrix $\mathbf{Z}_G$ at f_G, and the MAA is excited by an incident field. $\mathbf{Z}_A$ and $\mathbf{Z}_G$ are of size N by N. Let us use:

- P_{AAVG} to denote the average power available from the N-port generator, in CA (emission);
- P_{ARPA} to denote the average power received by the ports of the MAA, in CA (emission);
- P_{BAVA} to denote the average power available from the ports of the MAA, in CB (reception); and
- P_{BDPA} to denote the average power delivered by the ports of the MAA, in CB (reception).

We assume that $H(\mathbf{Z}_A)$ and $H(\mathbf{Z}_G)$ are positive definite so that, by Lemma 1, we can define $\mathbf{Y}_G = \mathbf{Z}_G^{-1}$ and $\mathbf{Y}_A = \mathbf{Z}_A^{-1}$, the hermitian parts of $\mathbf{Y}_G$ and $\mathbf{Y}_A$ being both positive definite. It also follows from Lemma 1 that, instead of assuming that $\mathbf{Z}_G$ and $\mathbf{Z}_A$ exist and that $H(\mathbf{Z}_G)$ and $H(\mathbf{Z}_A)$ are positive definite, we could equivalently have assumed that $\mathbf{Y}_G$ and $\mathbf{Y}_A$ exist and that $H(\mathbf{Y}_G)$ and $H(\mathbf{Y}_A)$ are positive definite.

To apply what was said in sections II to VI to the configurations shown in Fig. 4, we need to use $\mathbf{Z}_G = \mathbf{Z}_{GA}$; $\mathbf{Z}_A = \mathbf{Z}_{GB}$; $\mathbf{Y}_G = \mathbf{Y}_{GA}$; $\mathbf{Y}_A = \mathbf{Y}_{GB}$; $P_{ARPA} = P_{ADG}$; $P_{BAVA} = P_{BAVG}$ and $P_{BDPA} = P_{BDG}$. It follows that $t_A = P_{ARPA}/P_{AAVG}$ and $t_B = P_{BDPA}/P_{BAVA}$.

Let us use $\mathbf{I}_{SG}$ to denote the column vector of the rms short-circuit currents of the N-port generator in CA (emission). It follows from what was said in Section II that the set of the possible values of t_A is determined by $\mathbf{Y}_A$, $\mathbf{Y}_G$ and the set of the possible values of $\mathbf{I}_{SG}/||\mathbf{I}_{SG}||_2$ for $\mathbf{I}_{SG} \neq \mathbf{0}$, which is a subset of $\mathbb{S}_N$. If CA corresponds to an emission for MIMO radio transmission with rank-N spatial multiplexing, linearly independent signals are applied to the N ports of the MAA. Each of these signals is digitally modulated in such a way that it presents a suitable spectral efficiency, typically using pulse shaping and a multicarrier modulation such as OFDM [21]–[23]. In this case, it is reasonable to assume that, at a given time, $\mathbf{I}_{SG}/||\mathbf{I}_{SG}||_2$ may lie anywhere in $\mathbb{S}_N$.

Let us use $\mathbf{I}_{SA}$ to denote the column vector of the rms short-circuit currents of the MAA in CB (reception). It follows from what was said in Section II that the set of the possible values of t_B is determined by $\mathbf{Y}_A$, $\mathbf{Y}_G$ and the set of the possible values of $\mathbf{I}_{SA}/||\mathbf{I}_{SA}||_2$ for $\mathbf{I}_{SA} \neq \mathbf{0}$, which is a subset of $\mathbb{S}_N$. If CB corresponds to a reception of a signal intended for MIMO radio transmission with rank-N spatial multiplexing, and if the rank of the channel matrix is N, then linearly independent signals are delivered by the N ports of the MAA [24, Ch. 7]. In this case, if the channel matrix is well-conditioned, it may be reasonable to assume that, at a given time, $\mathbf{I}_{SA}/||\mathbf{I}_{SA}||_2$ may lie anywhere in $\mathbb{S}_N$.

B. MATCHING METRICS FOR AN N-PORT AND A MAA

In Section V.C and Section VI, we have already discussed the merits of F_M, F_R and the entries of $|\mathbf{S}|$ as matching metrics. The matching metric most commonly used by MAA designers is the entries of $|\mathbf{S}|$. However, other matching metrics or parameters are also used by MAA designers.

The active reflection coefficients (ARCs), denoted by $\Gamma^i_{\mathbf{a}}$ where $i \in \{1, \ldots, N\}$, and the total active reflection coefficient (TARC), denoted by $\Gamma^t_{\mathbf{a}}$, have been introduced some years ago [12]–[13]. Being functions of $\mathbf{a}$, they are not matching metrics as defined in Section V.C. According to the original definition of the TARC, we get $\Gamma^t_{\mathbf{a}} = r(\mathbf{a})$ in the special case of a lossless antenna [12]–[13]. Other authors use a different definition, according to which $\Gamma^t_{\mathbf{a}} = r(\mathbf{a})$ irrespective of antenna losses [14]–[15, Sec. 2.3.1].

The normalized total multiport reflectance defined and used in [16]–[17] is given by

$$\Gamma_{tot} = \sqrt{\frac{1}{N}\sum_{p=1}^{N}\sum_{q=1}^{N}|S_{pq}|^2} = \frac{1}{\sqrt{N}}||\mathbf{S}||_2 \,. \tag{62}$$

By (36) and (51), we find

$$0 \leqslant \frac{F_R}{\sqrt{N}} \leqslant \Gamma_{tot} \leqslant F_R \leqslant 1 \,. \tag{63}$$

Γ_{tot} is derived from $|\mathbf{S}|$. It corresponds to a wanted impedance matrix $\mathbf{Z}_W$ equal to $r_0 \mathbf{1}_N$ because the ideal value $\Gamma_{tot} = 0$ is obtained if and only if $\mathbf{Z}_A = r_0 \mathbf{1}_N$. Since it is a scalar, Γ_{tot} can be directly used to compare two N-ports MAAs. However, since the Frobenius norm is not an induced norm, Γ_{tot} does not have a direct physical meaning, like the ones revealed by (36) or (38) for F_R, or by (43) for F_M.

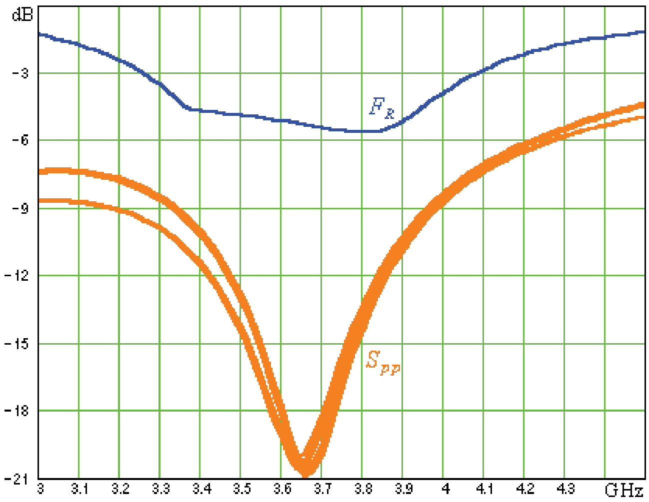

FIGURE 5. The return figure F_R and, for $p \in \{1, \ldots, 8\}$, the absolute value of the entry S_{pp} of $\mathbf{S}$, computed for the 8-port MAA considered in Section VII.

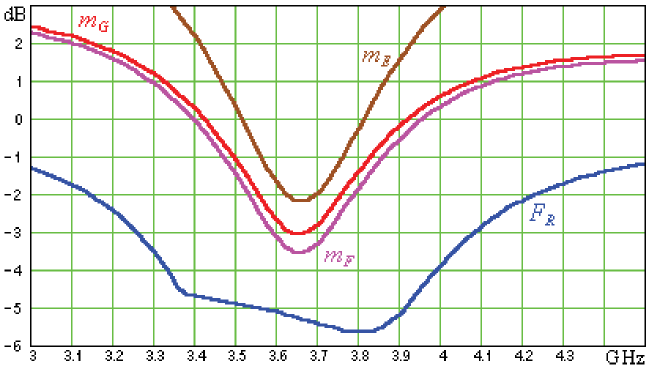

FIGURE 6. The return figure F_R and the upper bounds m_E, m_G and m_F, computed for the 8-port MAA considered in Section VII.

C. EXAMPLE

The article [25] presents a new self-decoupled 2-port antenna pair with shared radiator for 5G smartphones, and impressive results for an 8-port MAA comprising four 2-port antenna pairs, intended for the 3.3 GHz to 4.2 GHz frequency band. It includes many plots of simulated and measured $|S_{pq}|$, where S_{pq} is an entry of the scattering matrix $\mathbf{S}$ of the 8-port MAA, and where p and q lie in $\{1, \ldots, 8\}$.

The authors of [25] kindly provided the simulated S-parameters for their 8-port MAA, computed by utilizing the program HFSS. We used these S-parameters to compute the return figure F_R, shown with $|S_{1\,1}|$ to $|S_{8\,8}|$ in Fig. 5, for $r_0 = 50\,\Omega$. F_R was computed as $|||\mathbf{S}|||_2$ according to (36). We also computed F_M using (33) for $\mathbf{Z}_{GA} = r_0 \mathbf{1}_N$, and found that, within the computation accuracy, F_M is equal to F_R, in line with (42). Recall that, by (42) and (43), F_R is related to the minimum values of t_A and t_B obtained for $\mathbf{Z}_{GA} = r_0 \mathbf{1}_N$, so that F_R is meaningful for emission and for reception. In Fig. 5, each $|S_{p\,p}|$ is much less than F_R.

We also computed the upper bounds m_E, m_G and m_F, shown in Fig. 6 with F_R, for $r_0 = 50\,\Omega$. We observe that m_F is always less than m_E and m_G, but nevertheless substantially greater than F_R. Since m_F is the least of all

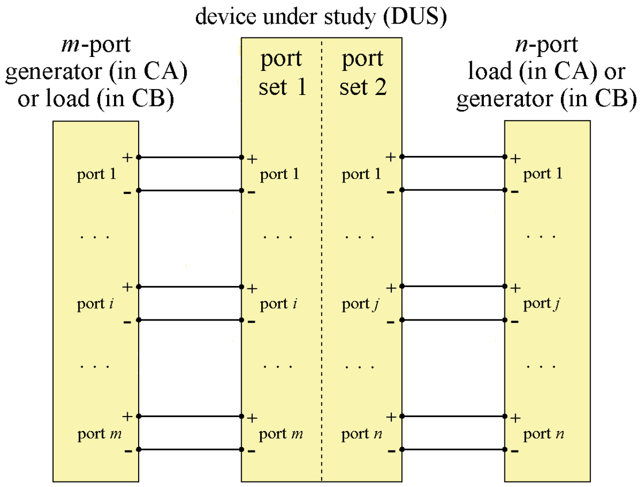

FIGURE 7. The two configurations, CA and CB, considered in Section VIII.

upper bounds only based on $|\mathbf{S}|$, this indicates that $|\mathbf{S}|$ does not allow an accurate evaluation of F_R. At some frequencies, m_F is greater than 0 dB, in which case we must conclude that $|\mathbf{S}|$ conveys no information at all on F_R.

In circumstances where the locations of $\mathbf{I}_{SG}/||\mathbf{I}_{SG}||_2$ and/or $\mathbf{I}_{SA}/||\mathbf{I}_{SA}||_2$ on $\mathbb{S}_N$ are not constant or not known, such as during MIMO radio transmission with spatial multiplexing, F_R characterizes the lowest possible power transfer ratios. Fig. 5 and Fig. 6 show that using the $|S_{pp}|$, or any upper bound on F_R only based on $|\mathbf{S}|$, is not satisfactory.

VIII. MORE THEORY FOR PASSIVE MIMO DEVICES

We consider two LTI circuits, referred to as "configurations", operating in the harmonic steady state, at the given frequency. The two configurations are shown in Fig. 7, which is identical to Fig. 7 of Part 1. All explanations concerning Fig. 7 of Part 1 are applicable to the configurations considered here. In Fig. 7, the device under study (DUS) is a MIMO device in the sense that: in configuration A (CA), the m ports of port set 1 are input ports and the n ports of port set 2 are output ports; and, in configuration B (CB), the n ports of port set 2 are input ports and the m ports of port set 1 are output ports.

As in Part 1, we assume that the DUS is passive; we use $\mathbf{Z}_{S1}$ to denote the impedance matrix of the m-port load or generator shown on the left in Fig. 7, $H(\mathbf{Z}_{S1})$ being positive definite; and we use $\mathbf{Z}_{S2}$ to denote the impedance matrix of the n-port load or generator shown on the right in Fig. 7, $H(\mathbf{Z}_{S2})$ being positive definite.

In addition, we assume that:

- if the DUS, the n-port load or generator shown on the right in Fig. 7 and the wires connecting them are regarded as an m-port load or generator (whose ports are the ports of port set 1), it has an impedance matrix denoted by $\mathbf{Z}_{T2}$, and $H(\mathbf{Z}_{T2})$ is positive definite; and
- if the DUS, the m-port load or generator shown on the left in Fig. 7 and the wires connecting them are regarded as an n-port load or generator (whose ports are the ports of port set 2), it has an impedance matrix denoted by $\mathbf{Z}_{T1}$, and $H(\mathbf{Z}_{T1})$ is positive definite.

We can utilize all results of sections II to V twice:

- a first time at port set 1, in which case we make use of $\mathbf{Z}_{GA} = \mathbf{Z}_{S1}$ and $\mathbf{Z}_{GB} = \mathbf{Z}_{T2}$ to define t_{A1} as t_A given by (14), t_{B1} as t_B given by (15), t_{MAX1} as the maximum value common to t_A and t_B according to (c) of Theorem 8, and t_{MIN1} as the minimum value common to t_A and t_B according to (d) of Theorem 8; and
- a second time at port set 2, in which case we make use of $\mathbf{Z}_{GA} = \mathbf{Z}_{T1}$ and $\mathbf{Z}_{GB} = \mathbf{Z}_{S2}$, to define t_{A2} as t_A given by (14), t_{B2} as t_B given by (15), t_{MAX2} as the maximum value common to t_A and t_B according to (c) of Theorem 8, and t_{MIN2} as the minimum value common to t_A and t_B according to (d) of Theorem 8.

Let us use:

- P_{AAVG1} to denote the average power available from the m-port generator connected to port set 1, in CA;
- P_{ARP1} to denote the average power received by port set 1 in CA (or, equivalently, the average power delivered by the m-port generator connected to port set 1 in CA);
- P_{AAVP2} to denote the average power available from port set 2, in CA;
- P_{ADP2} to denote the average power delivered by port set 2, in CA;
- P_{BAVG2} to denote the average power available from the n-port generator connected to port set 2, in CB;
- P_{BRP2} to denote the average power received by port set 2 in CB (or, equivalently, the average power delivered by the n-port generator connected to port set 2 in CB);
- P_{BAVP1} to denote the average power available from port set 1, in CB; and
- P_{BDP1} to denote the average power delivered by port set 1, in CB.

We have

$$t_{A1} = \frac{P_{ARP1}}{P_{AAVG1}}\,, \tag{64}$$

$$t_{A2} = \frac{P_{ADP2}}{P_{AAVP2}}\,, \tag{65}$$

$$t_{B1} = \frac{P_{BDP1}}{P_{BAVP1}}\,, \tag{66}$$

$$t_{B2} = \frac{P_{BRP2}}{P_{BAVG2}}\,. \tag{67}$$

The DUS being passive, the transducer power gain in CA is less than or equal to t_{A1}, and the transducer power gain in CB is less than or equal to t_{B2}. If the DUS is lossless, then the transducer power gain in CA is equal to t_{A1}, and the transducer power gain in CB is equal to t_{B2}.

Theorem 9. Let the DUS be a lossless and reciprocal device, and let both loads be reciprocal devices. We have

$$t_{MAX1} = t_{MAX2}\,. \tag{68}$$

In the case where $m = n$, we also have

$$t_{MIN1} = t_{MIN2}\,. \tag{69}$$

Proof: Let us assume that we are in CA. The DUS being passive and lossless, t_{A1} is the transducer power gain in CA, as defined in Theorem 4, which was stated and proven in Part 1. A comparison of Theorem 8 with Theorem 4 shows that t_{MAX1} and t_{MIN1} are the maximum value of the transducer power gain in CA and the minimum value of the transducer power gain in CA, respectively.

Let us now assume that we are in CB. The DUS being passive and lossless, t_{B2} is the transducer power gain in CB, as defined in Theorem 4. A comparison of Theorem 8 with Theorem 4 shows that t_{MAX2} and t_{MIN2} are the maximum value of the transducer power gain in CB and the minimum value of the transducer power gain in CB, respectively.

Based on the foregoing, the conclusion of Theorem 9 follows from (c) and (d) of Theorem 4. □

Theorem 10. Let the DUS be lossless. If the impedance matrix $\mathbf{Z}_{PAM12}$ defined in Section IV of Part 1 is of rank m, then

$$t_{MAX2} \geqslant t_{MAX1} \tag{70}$$

and

$$t_{MIN2} \leqslant t_{MIN1}\,. \tag{71}$$

If $\operatorname{rank} \mathbf{Z}_{PAM12} < n$, then

$$t_{MIN2} = 0\,. \tag{72}$$

If the impedance matrix $\mathbf{Z}_{PAM21}$ defined in Section IV of Part 1 is of rank n, then

$$t_{MAX1} \geqslant t_{MAX2} \tag{73}$$

and

$$t_{MIN1} \leqslant t_{MIN2}\,. \tag{74}$$

If $\operatorname{rank} \mathbf{Z}_{PAM21} < m$, then

$$t_{MIN1} = 0\,. \tag{75}$$

Proof: According to sections II and IV of Part 1, we know that the matrix $\mathbf{Z}_{PAM}$ is defined, and that it can be written in block form as in (32), the submatrices $\mathbf{Z}_{PAM11}$ of size m by m, $\mathbf{Z}_{PAM12}$ of size m by n, $\mathbf{Z}_{PAM21}$ of size n by m and $\mathbf{Z}_{PAM22}$ of size n by n being determined by the DUS, $\mathbf{Z}_{S1}$ and $\mathbf{Z}_{S2}$.

By Lemma 1, $H(\mathbf{Z}_{T1})$ being positive definite, $\mathbf{Z}_{T1}$ is invertible and $H(\mathbf{Z}_{T1}^{-1})$ is positive definite. Likewise, $H(\mathbf{Z}_{S2})$ being positive definite, $\mathbf{Z}_{S2}$ is invertible and $H(\mathbf{Z}_{S2}^{-1})$ is positive definite. Thus, $H(\mathbf{Z}_{T1}^{-1} + \mathbf{Z}_{S2}^{-1})$ is positive definite, so that $\mathbf{Z}_{T1}^{-1} + \mathbf{Z}_{S2}^{-1}$ is invertible and

$$\mathbf{Z}_{PAM22} = (\mathbf{Z}_{T1}^{-1} + \mathbf{Z}_{S2}^{-1})^{-1} \tag{76}$$

We use $\mathbf{I}_{S1}$ to denote the column vector of the rms short-circuit currents of the m-port generator connected to port set 1. In CA, if the DUS, the m-port generator shown on the left in Fig. 7 and the wires connecting them are regarded as an n-port generator, its impedance matrix is $\mathbf{Z}_{T1}$ as said above, and we use $\mathbf{I}_{T1}$ to denote the column vector of its rms short-circuit currents. By inspection and analysis, we find

$$\mathbf{I}_{T1} = \mathbf{Z}_{PAM22}^{-1} \mathbf{Z}_{PAM21} \mathbf{I}_{S1}\,, \tag{77}$$

in which we have used the fact that, by (76), $\mathbf{Z}_{PAM22}$ is invertible, and the fact that $\mathbf{Z}_{S2}$ is invertible.

In CA, for any $\mathbf{I}_{S1}$, we have $P_{ADP2} = P_{ARP1}$ and $P_{AAVP2} \leqslant P_{AAVG1}$, because the DUS is passive and lossless. $\mathbf{Z}_{T2}$ being determined only by the DUS and by $\mathbf{Z}_{S2}$, we can assume that we have chosen $\mathbf{Z}_{S1}$ in such a way that $\mathbf{Z}_{S1} = \mathbf{Z}_{T2}^*$. In this case, any excitation $\mathbf{I}_{S1}$ is such that $P_{ARP1} = P_{AAVG1}$. If we additionally assume that $\operatorname{rank} \mathbf{Z}_{PAM21} = n$, then, for any arbitrary nonzero $\mathbf{I}_{T1} \in \mathbb{C}^N$, there exists at least one nonzero excitation $\mathbf{I}_{S1}$ which satisfies (77). For such an excitation, we have $P_{ADP2} = P_{AAVG1}$, so that $P_{AAVP2} \geqslant P_{AAVG1}$. Thus, $P_{AAVP2} = P_{AAVG1}$ because we already know that we have $P_{AAVP2} \leqslant P_{AAVG1}$. Since we have found that, for any arbitrary nonzero $\mathbf{I}_{T1} \in \mathbb{C}^N$, we have $P_{ADP2} = P_{AAVP2}$, it follows from Remark 1 of [19] that $\mathbf{Z}_{S2} = \mathbf{Z}_{T1}^*$.

Let us no longer assume that $\mathbf{Z}_{S1} = \mathbf{Z}_{T2}^*$. We have just shown that, if $\operatorname{rank} \mathbf{Z}_{PAM21} = n$, then

$$(\mathbf{Z}_{S1} = \mathbf{Z}_{T2}^*) \Longrightarrow (\mathbf{Z}_{S2} = \mathbf{Z}_{T1}^*)\,. \tag{78}$$

Using the same approach in CB, we can prove that, if $\operatorname{rank} \mathbf{Z}_{PAM12} = m$, then

$$(\mathbf{Z}_{S2} = \mathbf{Z}_{T1}^*) \Longrightarrow (\mathbf{Z}_{S1} = \mathbf{Z}_{T2}^*)\,. \tag{79}$$

Let us assume that $\operatorname{rank} \mathbf{Z}_{PAM12} = m$. For any excitation $\mathbf{I}_{S1} \in \mathbb{C}^N$ in CA, the circumstance $\mathbf{Z}_{S2} = \mathbf{Z}_{T1}^*$ entails: $P_{ADP2} = P_{AAVP2}$; and $P_{ARP1} = P_{AAVG1}$ by (79). It follows from $P_{ADP2} = P_{ARP1}$ that, for said excitation, $P_{AAVP2} = P_{AAVG1}$. It must be stressed that this result is independent of the value of $\mathbf{Z}_{S2}$, because $\mathbf{Z}_{S2}$ has no effect on P_{AAVG1} and no effect on P_{AAVP2}. Thus, for any value of $\mathbf{Z}_{S2}$ and any excitation $\mathbf{I}_{S1} \in \mathbb{C}^N$ in CA, we have $t_{A1} = t_{A2}$ because $P_{ADP2} = P_{ARP1}$. Consequently, we obtain $t_{MAX2} \geqslant t_{MAX1}$ and $t_{MIN2} \leqslant t_{MIN1}$.

If, instead of assuming $\operatorname{rank} \mathbf{Z}_{PAM12} = m$, we assume that $\operatorname{rank} \mathbf{Z}_{PAM21} = n$ and consider CB, we likewise obtain $t_{MAX1} \geqslant t_{MAX2}$ and $t_{MIN1} \leqslant t_{MIN2}$.

In CA, if we assume that $\operatorname{rank} \mathbf{Z}_{PAM21} < m$, it follows from (77) and the rank-nullity theorem that there exists a nonzero excitation $\mathbf{I}_{S1}$ such that $\mathbf{I}_{T1} = \mathbf{0}$. In this case, we have $P_{ADP2} = P_{ARP1} = 0$, so that $t_{A1} = t_{A2} = 0$. It follows that $t_{MIN1} = 0$, but we cannot conclude anything about t_{MIN2}.

In CB, if we assume $\operatorname{rank} \mathbf{Z}_{PAM12} < n$, we likewise obtain $t_{MIN2} = 0$. □

Theorem 9 and Theorem 10 are new. However, (78) and (79) are not new, since several proofs of equivalent statements were published, for instance in Section III of [26] using scattering matrices, and in the Appendix of [27] using the admittance matrix of the DUS. The proof of (78) and (79) shown above is new, and particularly simple and concise.

Theorem 11. We assume that the DUS is lossless, and $n = m$. Let $F_{M1} = \sqrt{1 - t_{MIN1}}$ be the power match figure at port set 1, and $F_{M2} = \sqrt{1 - t_{MIN2}}$ be the power match figure at port set 2. We have

$$F_{M1} = F_{M2}\,. \tag{80}$$

If $\operatorname{rank} \mathbf{Z}_{PAM12} < m = n$ or $\operatorname{rank} \mathbf{Z}_{PAM21} < m = n$, then

$$F_{M1} = F_{M2} = 1\,. \tag{81}$$

Proof: If $\operatorname{rank} \mathbf{Z}_{PAM12} = \operatorname{rank} \mathbf{Z}_{PAM21} = m = n$, the result $F_{M1} = F_{M2}$ follows from (71) and (74). If $\operatorname{rank} \mathbf{Z}_{PAM12} < m = n$ and $\operatorname{rank} \mathbf{Z}_{PAM21} < m = n$, the result $F_{M1} = F_{M2} = 1$ follows from (72) and (75).

If $\operatorname{rank} \mathbf{Z}_{PAM21} < \operatorname{rank} \mathbf{Z}_{PAM12} = m = n$, we have $t_{MIN1} = 0$ by (75) and $t_{MIN2} \leqslant t_{MIN1}$ by (71), so that $t_{MIN2} = t_{MIN1} = 0$ and $F_{M1} = F_{M2} = 1$

If $\operatorname{rank} \mathbf{Z}_{PAM12} < \operatorname{rank} \mathbf{Z}_{PAM21} = m = n$, we have $t_{MIN2} = 0$ by (72) and $t_{MIN1} \leqslant t_{MIN2}$ by (74), so that $t_{MIN2} = t_{MIN1} = 0$ and $F_{M1} = F_{M2} = 1$. □

IX. EXAMPLES INVOLVING PASSIVE MIMO DEVICES

A. FIRST EXAMPLE

In a first example such that $m = n = 2$, $\mathbf{Z}_{S1}$ is equal to $\mathbf{Z}_{GA}$ given by (30) and $\mathbf{Z}_{S2}$ is equal to $\mathbf{Z}_{GB}$ given by (31). We assume that the DUS has an impedance matrix given by

$$\mathbf{Z} = \begin{pmatrix} 25j & 31+11j & 31+5j & 17+40j \\ -31+11j & 35j & 3+62j & 40+17j \\ -31+5j & -3+62j & 41j & 21+49j \\ -17+40j & -40+17j & -21+49j & 21j \end{pmatrix} \Omega\,. \tag{82}$$

$\mathbf{Z}_{S1}$, $\mathbf{Z}_{S2}$ and $\mathbf{Z}$ are not symmetric. $\mathbf{Z}_{S1}$ and $\mathbf{Z}_{S2}$ have each a positive definite hermitian part. We have $H(\mathbf{Z}) = 0$ because $\mathbf{Z}$ is the impedance matrix of a lossless DUT.

We have computed $\mathbf{Z}_{PAM}$ and found that $\operatorname{rank} \mathbf{Z}_{PAM12} = \operatorname{rank} \mathbf{Z}_{PAM21} = 2$. F_{M1} and F_{M2} have been computed by utilizing Theorem 7 and (33), at port set 1 and at port set 2. The results are $F_{M1} \simeq 0.964873$ and $F_{M2} \simeq 0.964873$. These results are compatible with Theorem 11.

B. SECOND EXAMPLE

In a second example such that $m = n = 2$, $\mathbf{Z}_{S1}$ and $\mathbf{Z}_{S2}$ are the same as in the first example. We assume that the DUS has an impedance matrix given by

$$\mathbf{Z} = \begin{pmatrix} 25j & 31+11j & 31+5j & 62+10j \\ -31+11j & 35j & 3+49j & 6+98j \\ -31+5j & -3+49j & 41j & 21+49j \\ -62+10j & -6+98j & -21+49j & 21j \end{pmatrix} \Omega\,. \tag{83}$$

$\mathbf{Z}$ is not symmetric, and $H(\mathbf{Z}) = 0$ because $\mathbf{Z}$ is the impedance matrix of a lossless DUT.

We have computed $\mathbf{Z}_{PAM}$ and found that $\operatorname{rank} \mathbf{Z}_{PAM12} = \operatorname{rank} \mathbf{Z}_{PAM21} = 1$. F_{M1} and F_{M2} have been computed by utilizing Theorem 7 and (33), at port set 1 and at port set 2. The results are $F_{M1} \simeq 1.000000$ and $F_{M2} \simeq 1.000000$. These results are compatible with Theorem 11.

C. THIRD EXAMPLE

In a third example such that $m = n = 2$, $\mathbf{Z}_{S1}$ and $\mathbf{Z}_{S2}$ are the same as in the first example. We assume that the DUS has an impedance matrix given by

$$\mathbf{Z} = \begin{pmatrix} 25j & 31+11j & 0 & 0 \\ -31+11j & 35j & 0 & 0 \\ 0 & 0 & 41j & 21+49j \\ 0 & 0 & -21+49j & 21j \end{pmatrix} \Omega\,. \tag{84}$$

$\mathbf{Z}$ is not symmetric, and $H(\mathbf{Z}) = 0$ because $\mathbf{Z}$ is the impedance matrix of a lossless DUT.

We have computed $\mathbf{Z}_{PAM}$ and found that $\mathbf{Z}_{PAM12} = \mathbf{Z}_{PAM21} = \mathbf{0}$, so that $\operatorname{rank} \mathbf{Z}_{PAM12} = \operatorname{rank} \mathbf{Z}_{PAM21} = 0$. F_{M1} and F_{M2} have been computed by utilizing Theorem 7 and (33). The results $F_{M1} \simeq 1.000000$ and $F_{M2} \simeq 1.000000$ are compatible with Theorem 11.

X. CONCLUSION

We have stated and proven a new reciprocal theorem on the power transfer ratios between two passive multiport devices. This theorem is reciprocal in the sense that it relates the power transfer ratio t_A to the power transfer ratio t_B. However, this theorem does not assume that $\mathbf{Z}_{GA}$ and $\mathbf{Z}_{GB}$ are symmetric. That is, it does not assume that the N-port load used in CA or the N-port load used in CB satisfy the relations stated in the conclusion of the classical reciprocity theorem, as for instance set forth in [4, Ch. 16] and [28, Ch. 1].

We have used the reciprocal theorem on the power transfer ratios to define the power match figure F_M from the minimum values of t_A or t_B. F_M is a metric of the power transfer ratios. It is relevant to all situations in which the location of $\mathbf{I}_{SGA}/||\mathbf{I}_{SGA}||_2$ on $\mathbb{S}_N$ is not constant or not known, or in which the location of $\mathbf{I}_{SGB}/||\mathbf{I}_{SGB}||_2$ on $\mathbb{S}_N$ is not constant or not known.

In the case where the ports of the N-port generator used in CA, or of the N-port load used in CB, are uncoupled and present the same real impedance r_0, we have shown that F_M is equal to the return figure F_R determined for the reference resistance r_0. In this case, we have explained that, in contrast to F_R, the absolute values of the entries S_{pq} of $\mathbf{S}$ do not sufficiently characterize the power transfer ratio in CA, when the location of $\mathbf{I}_{SGA}/||\mathbf{I}_{SGA}||_2$ on $\mathbb{S}_N$ is not constant or not known. This result might look more surprising if we phrase it: "the phases of the entries of the scattering matrix have an influence on the power transfer ratios".

We have looked at the special case in which one of the two passive multiport devices is a multiport antenna array (MAA). In this case, CA may correspond to emission, and CB to reception. We have explained why F_M or F_R should be considered as matching metrics or design parameters for a MAA used for MIMO radio transmission using spatial multiplexing. F_R may advantageously be used to specify and characterize the MAA. Any monotone function of F_R is often a good choice of performance parameter for designing and optimizing a MAA, adjusting a decoupling and matching circuit of the MAA, and automatically adjusting a multiple-antenna-port antenna tuner for the MAA [11].

We have also looked at the power transfer ratios occurring at each side of a passive MIMO device. We have established several theorems applicable to the case in which the MIMO device is lossless. This case is relevant to ideal decoupling and matching circuits, and to ideal antenna tuners.

APPENDIX A

For the single-port generators and the single-port loads considered in Section I, in CA, the power reflection coefficient defined in [6, Sec. III] is given by

$$\rho_P = \left| \frac{Z_{GB} - \overline{Z_{GA}}}{Z_{GA} + Z_{GB}} \right|^2 . \tag{85}$$

It is the squared absolute value of the power-wave reflection coefficient used by numerous authors [6, Sec. III], [29, Sec. 4.3], [30, Sec. 1.7]. By (85), we get

$$\rho_P = \frac{[\mathrm{Re}(Z_{GB}) - \mathrm{Re}(Z_{GA})]^2 + [\mathrm{Im}(Z_{GB}) + \mathrm{Im}(Z_{GA})]^2}{|Z_{GA} + Z_{GB}|^2} , \tag{86}$$

and then

$$\rho_P = 1 - \frac{4\mathrm{Re}(Z_{GA})\mathrm{Re}(Z_{GB})}{|Z_{GA} + Z_{GB}|^2} = 1 - t_A . \tag{87}$$

In [6, Sec. III], the power transmission coefficient in CA is defined as $1 - \rho_P$, so that by (87) it is equal to t_A. Likewise, the power transmission coefficient in CB is equal to t_B.

APPENDIX B

Let n be a positive integer. Let $\mathbf{A}$ and $\mathbf{B}$ be two square complex matrices of size n by n, such that $\mathbf{A} + \mathbf{B}$ is invertible. We want to prove that $\mathbf{K}$ defined by (16) and $\mathbf{L}$ defined by (17) have the same characteristic polynomial.

Proof: Using $\mathbf{C} = (\mathbf{A} + \mathbf{B})^{-1}$, (16) and (17) may be written

$$\mathbf{K} = \mathbf{C}^*(\mathbf{A} + \mathbf{A}^*)\mathbf{C}(\mathbf{B} + \mathbf{B}^*) \tag{88}$$

and

$$\mathbf{L} = \mathbf{C}^*(\mathbf{B} + \mathbf{B}^*)\mathbf{C}(\mathbf{A} + \mathbf{A}^*) . \tag{89}$$

Using $\mathbf{C}(\mathbf{A} + \mathbf{B}) = \mathbf{1}_n = (\mathbf{A} + \mathbf{B})\mathbf{C}$ and (88), we get

$$\mathbf{K} = (\mathbf{1}_n + \mathbf{C}^*\mathbf{A} - \mathbf{C}^*\mathbf{B}^*)(\mathbf{1}_n + \mathbf{C}\mathbf{B}^* - \mathbf{C}\mathbf{A}) \tag{90}$$

from which we obtain

$$\begin{aligned} \mathbf{K} = \mathbf{C}^*(\mathbf{A} - \mathbf{B}^*)\mathbf{C}(\mathbf{B}^* - \mathbf{A}) \\ + \mathbf{C}^*(\mathbf{A} - \mathbf{B}^*) + \mathbf{C}(\mathbf{B}^* - \mathbf{A}) + \mathbf{1}_n . \end{aligned} \tag{91}$$

Thus, we have

$$\mathbf{K} = [\mathbf{C}^*(\mathbf{A} - \mathbf{B}^*)\mathbf{C} - \mathbf{C}^* + \mathbf{C}](\mathbf{B}^* - \mathbf{A}) + \mathbf{1}_n . \tag{92}$$

Likewise, using (88), we get

$$\mathbf{L} = [\mathbf{C}^*(\mathbf{B} - \mathbf{A}^*)\mathbf{C} - \mathbf{C}^* + \mathbf{C}](\mathbf{A}^* - \mathbf{B}) + \mathbf{1}_n . \tag{93}$$

Let us now study $\mathbf{K}^*$. Using (88), we obtain

$$\mathbf{K}^* = (\mathbf{B} + \mathbf{B}^*)\mathbf{C}^*(\mathbf{A} + \mathbf{A}^*)\mathbf{C} . \tag{94}$$

It follows from [18, Sec. 1.3.22] that $\mathbf{K}^*$ has the same eigenvalues, counting multiplicities, as

$$\mathbf{J} = \mathbf{C}^*(\mathbf{A} + \mathbf{A}^*)\mathbf{C}(\mathbf{B} + \mathbf{B}^*) . \tag{95}$$

A comparison of (88) and (95) shows that $\mathbf{J} = \mathbf{K}$. It follows that $\mathbf{K}$ and $\mathbf{K}^*$ have the same eigenvalues, counting multiplicities. Using (92), we obtain

$$\mathbf{K}^* = (\mathbf{B} - \mathbf{A}^*)[\mathbf{C}^*(\mathbf{A}^* - \mathbf{B})\mathbf{C} - \mathbf{C} + \mathbf{C}^*] + \mathbf{1}_n , \tag{96}$$

which leads us to

$$\mathbf{K}^* = (\mathbf{A}^* - \mathbf{B})[\mathbf{C}^*(\mathbf{B} - \mathbf{A}^*)\mathbf{C} - \mathbf{C}^* + \mathbf{C}] + \mathbf{1}_n . \tag{97}$$

Let $\mathbf{X} = \mathbf{A}^* - \mathbf{B}$ and $\mathbf{Y} = \mathbf{C}^*(\mathbf{B} - \mathbf{A}^*)\mathbf{C} - \mathbf{C}^* + \mathbf{C}$. Consider the following identities involving bloc matrices of size n by n:

$$\begin{aligned} &\begin{pmatrix} \mathbf{XY} + \mathbf{1}_n & \mathbf{0} \\ \mathbf{Y} & \mathbf{1}_n \end{pmatrix} \begin{pmatrix} \mathbf{1}_n & \mathbf{X} \\ \mathbf{0} & \mathbf{1}_n \end{pmatrix} \\ &\qquad = \begin{pmatrix} \mathbf{XY} + \mathbf{1}_n & \mathbf{XYX} + \mathbf{X} \\ \mathbf{Y} & \mathbf{YX} + \mathbf{1}_n \end{pmatrix} , \end{aligned} \tag{98}$$

and

$$\begin{aligned} &\begin{pmatrix} \mathbf{1}_n & \mathbf{X} \\ \mathbf{0} & \mathbf{1}_n \end{pmatrix} \begin{pmatrix} \mathbf{1}_n & \mathbf{0} \\ \mathbf{Y} & \mathbf{YX} + \mathbf{1}_n \end{pmatrix} \\ &\qquad = \begin{pmatrix} \mathbf{XY} + \mathbf{1}_n & \mathbf{XYX} + \mathbf{X} \\ \mathbf{Y} & \mathbf{YX} + \mathbf{1}_n \end{pmatrix} . \end{aligned} \tag{99}$$

The factor

$$\mathbf{Z} = \begin{pmatrix} \mathbf{1}_n & \mathbf{X} \\ \mathbf{0} & \mathbf{1}_n \end{pmatrix} \tag{100}$$

which appears in the left-hand side of (98) and in the left-hand side of (99) is invertible since its determinant is 1. Thus, we may invert it and conclude that

$$\mathbf{Z}^{-1} \begin{pmatrix} \mathbf{XY} + \mathbf{1}_n & \mathbf{0} \\ \mathbf{Y} & \mathbf{1}_n \end{pmatrix} \mathbf{Z} = \begin{pmatrix} \mathbf{1}_n & \mathbf{0} \\ \mathbf{Y} & \mathbf{YX} + \mathbf{1}_n \end{pmatrix} . \tag{101}$$

It follows that the matrices

$$\mathbf{D}_1 = \begin{pmatrix} \mathbf{XY} + \mathbf{1}_n & \mathbf{0} \\ \mathbf{Y} & \mathbf{1}_n \end{pmatrix} \tag{102}$$

and

$$\mathbf{D}_2 = \begin{pmatrix} \mathbf{1}_n & \mathbf{0} \\ \mathbf{Y} & \mathbf{YX} + \mathbf{1}_n \end{pmatrix} \tag{103}$$

are similar. The eigenvalues of $\mathbf{D}_1$ are the eigenvalues of $\mathbf{XY} + \mathbf{1}_n$ together with n ones. The eigenvalues of $\mathbf{D}_2$ are the eigenvalues of $\mathbf{YX} + \mathbf{1}_n$ together with n ones. Since, by [18, Sec. 1.3.4], $\mathbf{D}_1$ and $\mathbf{D}_2$ have the same eigenvalues, counting multiplicities, it follows that $\mathbf{XY} + \mathbf{1}_n$ and $\mathbf{YX} + \mathbf{1}_n$ have the same eigenvalues, counting multiplicities.

By (97), we have $\mathbf{K}^* = \mathbf{XY} + \mathbf{1}_n$, and by (93), we have $\mathbf{L} = \mathbf{YX} + \mathbf{1}_n$. Having already established that $\mathbf{K}$ and $\mathbf{K}^*$ have the same eigenvalues, counting multiplicities, we may conclude that $\mathbf{K}$ and $\mathbf{L}$ have the same eigenvalues, counting multiplicities. □

ACKNOWLEDGMENT

The authors would like to thank Libin Sun and Prof. Zhijun Zhang, both of Tsinghua University in Beijing, China, for kindly providing the data used above in Section VII.C, concerning the 8-port MAA disclosed in [25].

REFERENCES

[1] F. Broydé and E. Clavelier, "Some Results on Power in Passive Linear Time-Invariant Multiports, Part 1," *Excem Research Papers in Electronics and Electromagnetics*, no. 2, Jan. 2021.

[2] F. Broydé and E. Clavelier, "Two reciprocal power theorems for passive linear time-invariant multiports," *IEEE Trans. Circuits Syst. I: Reg. Papers*, vol. 67, No. 1, pp. 86-97, Jan. 2020.

[3] F. Broydé and E. Clavelier, "Corrections to 'Two reciprocal power theorems for passive linear time-invariant multiports'," *IEEE Trans. Circuits Syst. I: Reg. Papers*, vol. 67, no. 7, pp. 2516-2517, Jul. 2020.

[4] C.A. Desoer and E.S. Kuh, *Basic Circuit Theory*, New York, NY, USA: McGraw-Hill, 1969.

[5] W.L. Everitt and G.E. Anner, *Communication Engineering*, 3rd ed., New York, NY, USA: McGraw-Hill, 1956.

[6] K. Kurokawa, "Power waves and the scattering matrix," *IEEE Trans. on Microw. Theory Techn.*, vol. 13, no. 2, pp. 194-202, Mar. 1965.

[7] F. Broydé and E. Clavelier, "A new multiple-antenna-port and multiple-user-port antenna tuner," *Proc. 2015 IEEE Radio & Wireless Week, RWW 2015*, pp. 41-43, Jan. 2015.

[8] F. Broydé and E. Clavelier, "Some properties of multiple-antenna-port and multiple-user-port antenna tuners," *IEEE Trans. Circuits Syst. I, Reg. Papers*, vol. 62, no. 2, pp. 423-432, Feb. 2015.

[9] F. Broydé and E. Clavelier, "Two multiple-antenna-port and multiple-user-port antenna tuners," *Proc. 9th European Conference on Antennas and Propagation*, EuCAP 2015, pp. 1-5, Apr. 2015.

[10] F. Broydé and E. Clavelier, "A tuning computation technique for a multiple-antenna-port and multiple-user-port antenna tuner," *Int. Journal of Antennas and Propagation*, vol. 2016, Article ID 4758486, Nov. 2016.

[11] F. Broydé and E. Clavelier, "A typology of antenna tuner control schemes, for one or more antennas," *Excem Research Papers in Electronics and Electromagnetics*, no. 1, Jun. 2020.

[12] M. Manteghi and Y. Rahmat-Samii, "Broadband characterization of the total active reflection coefficient of multiport antennas," *2003 IEEE Antennas and Propagation Society Int. Symp. Digest*, vol. 3, pp. 20-23, Jun. 2003.

[13] M. Manteghi and Y. Rahmat-Samii, "Multiport characteristics of a wide-band cavity backed annular patch antenna for multipolarization operations," *IEEE Trans. Antennas Propag.*, vol. 53, no. 1, pp. 466-474, Jan. 2005.

[14] S. Su, C. Lee and F. Chang, "Printed MIMO-antenna system using neutralization-line technique for wireless USB-dongle applications," *IEEE Trans. Antennas Propag.*, vol. 60, no. 2, pp. 456-463, Feb. 2012.

[15] M.S. Sharawi, *Printed MIMO antenna engineering*, Norwood, MA, USA: Artech House, 2014.

[16] W.L. Schroeder and A. Krewski, "Total multi-port return loss as a figure of merit for MIMO antenna systems," *Proc. of the 3rd European Wireless Technology Conference*, EuWiT 2010, pp. 265-268, Sep. 2010.

[17] A. Krewski, W.L. Schroeder and K. Solbach, "Matching network synthesis for mobile MIMO antennas based on minimization of the total multi-port reflectance," *Proc. of the 2011 Loughborough Antennas and Propagation Conference*, LAPC 2011, pp. 1-4, Nov. 2011.

[18] R.A. Horn and C.R. Johnson, *Matrix analysis*, 2nd ed., New York, NY, USA: Cambridge University Press, 2013.

[19] C.A. Desoer, "The maximum power transfer theorem for n-ports," *IEEE Trans. Circuit Theory*, vol. 20, no. 3, pp. 328-330, May 1973.

[20] H.P. Westman, Ed., *Reference Data for Radio Engineers*, 5th ed., Indianapolis, IN, USA: Howard W. Sams & Co., 1968.

[21] J.G. Proakis and M. Salehi, *Digital Communications*, 5th ed., New York, NY, USA: McGraw-Hill, 2008.

[22] B. Dahlman, S. Parkvall and J. Sköld, *4G LTE/LTE-Advanced for Mobile Broadband*, Amsterdam, Netherlands: Elsevier, 2011.

[23] B. Clerckx and C. Oestges, *MIMO Wireless Networks*, 2nd ed., Amsterdam, Netherlands: Elsevier, 2013.

[24] D. Tse and P. Viswanath, *Fundamentals of Wireless Communication*, New York, NY, USA: Cambridge University Press, 2005.

[25] L. Sun, Y. Li, Z. Zhang and H. Wang, "Self-decoupled MIMO antenna pair with shared radiator for 5G smartphones," *IEEE Trans. Antennas Propag.*, vol. 68, no. 5, pp. 3423-3432, May 2020.

[26] J.W. Wallace and M.A. Jensen, "Termination-dependent diversity performance of coupled antennas: network theory analysis," *IEEE Trans. Antennas Propag.*, vol. 52, no. 1, pp. 98-105, Jan. 2004.

[27] F. Broydé and E. Clavelier, "The noise performance of a multiple-input-port and multiple-output-port low-noise amplifier connected to an array of coupled antennas," *Int. Journal of Antennas and Propagation*, vol. 2011, Article ID 438478, Nov. 2011.

[28] E.S. Kuh and R.A. Rohrer, *Theory of Linear Active Networks*, San Francisco, CA, USA: Holden-Day, 1967.

[29] D.M. Pozar, *Microwave Engineering*, 4th ed., Hoboken, NJ, USA: John Wiley & Sons, 2012.

[30] G. Gonzalez, *Microwave Transistor Amplifiers*, 2nd ed., Upper Saddle River, NJ, USA: Prentice Hall, 1984.

FRÉDÉRIC BROYDÉ was born in France in 1960. He received the M.S. degree in physics engineering from the Ecole Nationale Supérieure d'Ingénieurs Electriciens de Grenoble (ENSIEG) and the Ph.D. in microwaves and microtechnologies from the Université des Sciences et Technologies de Lille (USTL).

He co-founded the Excem corporation in May 1988, a company providing engineering and research and development services. He is president and CTO of Excem. Most of his activity is allocated to engineering and research in electronics, radio, antennas, electromagnetic compatibility (EMC) and signal integrity.

Dr. Broydé is author or co-author of about 100 technical papers, and inventor or co-inventor of about 80 patent families, for which 48 US patents have been granted. He is a Senior Member of the IEEE since 2001. He is a licensed radio amateur (F5OYE).

EVELYNE CLAVELIER was born in France in 1961. She received the M.S. degree in physics engineering from the Ecole Nationale Supérieure d'Ingénieurs Electriciens de Grenoble (ENSIEG).

She is co-founder of the Excem corporation, based in Maule, France. She is CEO of Excem. She is also President of Eurexcem (a subsidiary of Excem) and President of Tekcem, a company selling or licensing intellectual property rights to foster research. She is also an active engineer and researcher. Her current research areas are radio communications and circuit theory.

Prior to starting Excem in 1988, she worked for Schneider Electrics (in Grenoble, France), STMicroelectronics (in Grenoble, France), and Signetics (in Mountain View, USA).

Ms. Clavelier is the author or a co-author of about 80 technical papers. She is co-inventor of about 80 patent families. She is a Senior Member of the IEEE since 2002. She is a licensed radio amateur (F1PHQ).